Spring 2019

Impacts of Major Freshwater Ions on the Acute Toxicity and Chemical Behavior of Silver Nanoparticles

Claire A. Walli
Western Washington University, claire.walli@gmail.com

Impacts of Major Freshwater Ions on the Acute Toxicity and Chemical Behavior of Silver Nanoparticles

By

Claire A. Walli

Accepted in Partial Completion
of the Requirements for the Degree
Master of Science

ADVISORY COMMITTEE

Chair, Dr. Ruth Sofield

Dr. Brian Bingham

Dr. Steven Emory

GRADUATE SCHOOL

Kathleen L. Kitto, Acting Dean

Master's Thesis

In presenting this thesis in partial fulfillment of the requirements for a master's degree at Western Washington University, I grant to Western Washington University the non-exclusive royalty-free right to archive, reproduce, distribute, and display the thesis in any and all forms, including electronic format, via any digital library mechanisms maintained by WWU.

I represent and warrant this is my original work, and does not infringe or violate any rights of others. I warrant that I have obtained written permissions from the owner of any third party copyrighted material included in these files.

I acknowledge that I retain ownership rights to the copyright of this work, including but not limited to the right to use all or part of this work in future works, such as articles or books.

Library users are granted permission for individual, research and non-commercial reproduction of this work for educational purposes only. Any further digital posting of this document requires specific permission from the author.

Any copying or publication of this thesis for commercial purposes, or for financial gain, is not allowed without my written.

Claire A. Walli

May 31, 2019

Impacts of Major Freshwater Ions on the Acute Toxicity and Chemical Behavior of Silver Nanoparticles

A Thesis
Presented to
The Faculty of
Western Washington University

In Partial Fulfillment
Of the Requirements for the Degree
Master of Science

By
Claire A. Walli
May 2019

Abstract

Silver nanoparticles (AgNPs) are increasing in presence in commercial and medical products due to their bactericidal properties and can be transported into the environment during the laundering, use, and waste of those products. Strong evidence suggests aqueous silver (Ag^+) dissolved from the AgNP surface is the toxic component of AgNPs but there is no consensus on the possibility of additional nanoparticle-specific properties that elicit toxicity. Ag^+ toxicity to freshwater organisms has been well studied using the Biotic Ligand Model (BLM), which describes how water quality conditions, such as the concentrations of certain freshwater ions, affect the toxicity of Ag^+. Some freshwater ions also cause AgNPs to aggregate, which can reduce the surface area from which Ag^+ can dissolve. The sensitivity of AgNPs to water quality conditions has made studying their toxicity challenging in part because the range of acceptable water quality conditions in standardized toxicity testing methods produces different AgNP toxicity results.

This study assessed the impacts of the freshwater ions Ca^{2+}, Na^+, Cl^-, and SO_4^{2-} on AgNP toxicity and chemical behavior in ASTM acute *Daphnia magna* toxicity testing conditions. Toxicity and analytical tests were performed in experimental waters created by adding fixed concentrations of NaCl, $CaCl_2$, and Na_2SO_4 to ASTM moderately hard water (MHW) in a factorial design. AgNP sedimentation was measured using UV-Vis, and particle size distribution and particle concentration were measured using the single particle ICP-MS technique. LC50s for experimental waters ranged from 53.48 – 383.52 µg/L. NaCl and $CaCl_2$ reduced toxicity in comparison to MHW. The rank order for AgNP LC50s in the experimental waters was the same as the rank order that the BLM predicted for Ag^+ toxicity indicating that Ag^+ dissolved from the AgNP may have been responsible for some of the AgNP toxicity. However, $CaCl_2$ reduced toxicity more than the BLM predicted should happen based on Ag^+ and there was a much larger interaction effect between $CaCl_2$ and NaCl than was predicted. $CaCl_2$ significantly increased particle size and sedimentation rates, which was concluded to be caused by the Ca^{2+}. An interaction effect between $CaCl_2$ and NaCl was also observed for sedimentation, which appeared to be due to the doubled Cl^- concentration. AgNP aggregation was likely responsible for the differences between the AgNP toxicity results and the predictions of the BLM supporting that the BLM is not able to completely characterize all of the factors that affect AgNP toxicity.

Acknowledgements

Many thanks are owed to the large group of people who helped this thesis come to fruition. First to my thesis advisor, Dr. Ruth Sofield, for the opportunity to take on this project and for her guidance through the seemingly endless twists and turns that this project took from start to finish. Thanks to the other faculty on my committee: Dr. Brian Bingham for his perspective and suggestions on appropriate statistical tools to apply to unusual analyses, and Dr. Steve Emory for getting the ball rolling on how to think about nanoparticle chemistry. Thanks also to Dr. Robin Matthews for her guidance and support over the course of this project.

I began this project as a novice at analytical chemistry and my now versatile skillset can be attributed to many: Kyle Mikkelson in AMSEC, Dr. Manual Montaño, and Ed Bain for their practical experience on the ICP-MS and with the single particle technique; Dan Carnevale and Charles Wandler in Scientific Technical Services for instrumentation assistance on the UV-Vis and HPLC; Sam Danforth for helping with DLS and the ultracentrifuge; and Scott Wilkinson and Michael Hilles for their unending general laboratory support. Thanks also to Robert Santore for his expertise troubleshooting the Biotic Ligand Model. Considerable thanks to Huxley College of the Environment and Western Washington University for providing the funding that made running all of the lab work for this project possible.

Thank you to the handful of undergraduate research assistants who dedicated considerable time to learn methods and run tests for this study: Tabitha Bergevin-Krumme, Miranda Aiken, Austin Faccone, and Winston Booth. The sheer volume of this project was accomplished because of their efforts. Finally, thanks especially to Gunnar Guddal, Eric Lawrence, and Ian Moran for the time they donated to help me run toxicity tests, brainstorm methods, and constantly remind me why I love science and toxicology.

Table of Contents

List of Tables

List of Figures

Introduction

Nanomaterials are any solid material with at least a single dimension between 1 – 100 nm (Fabrega et al. 2011; Harmon et al. 2014). The extremely high surface area to mass ratio that objects in the nanoscale possess gives them unique properties that can deviate substantially from the properties of their parent bulk materials (Meesters et al. 2013). Manufactured nanomaterials, referred to as engineered nanomaterials (ENMs), are increasing in commercial use across the globe. In this category, silver nanoparticles (AgNPs) are the most commercially used (Fabrega et al. 2011; Lorenz et al. 2012). AgNPs are included in "colloidal silver", which has a history of medical applications (Roe 1915) and is still used today as a homeopathic treatment (Chikramane et al. 2017). Although information is surfacing about the human health risk of AgNP exposure (Schäfer et al. 2013), the antimicrobial properties of AgNPs (Gao et al. 2009; Sharma et al. 2009; Xiu et al. 2012; Loza et al. 2014) and their relatively low human toxicity—particularly from dermal exposure (Schäfer et al. 2013)—make them an attractive chemical for consumer products such as textiles, medical equipment, food storage containers, and personal care products (Hicks et al. 2015; Limpiteepraken and Babel 2016). The laundering, use, and disposal of these products transports AgNPs into wastewater treatment facilities where they are not completely removed (Mitrano et al. 2012), and eventually to the environment via wastewater effluent.

The environmental toxicity of dissolved ionic silver (Ag^+), which can be released from AgNPs, is well understood using a conceptual model known as the Biotic Ligand Model (BLM) (Di Toro et al. 2001; Bielmeyer et al. 2007). The BLM calculates the speciation and predicts the aquatic toxicity of certain metals to aquatic organisms based on the

modeled concentration of metal on the organism's "biotic ligand", which refers to the toxic site of action. The BLM accounts for water quality conditions that can alter metal toxicity through a variety of mechanisms: cations such as Ca^{2+} or Na^{+} compete with the metal ion (referred to hereafter in the context of Ag^{+}) for binding sites at the biotic ligand, which reduces the accumulated Ag^{+} concentration; inorganic anions in solution form ligands with Ag^{+}, notably Cl^{-} precipitates with Ag^{+} and forms $AgCl_{(s)}$ and various additional dissolved AgCl species, reducing the bioavailability of Ag^{+}. The BLM was designed specifically for aqueous metals but has been used to explore the toxicity of metallic ENMs based on the predicted toxicity of their dissolved constituents (Li et al. 2013; Khan et al. 2015; Sakamoto et al. 2015).

Dissolved Ag^{+} from the AgNP surface has been shown to play a significant role in AgNP toxicity (Kennedy et al. 2010; Li and Lenhart 2012; Harmon et al. 2014; Groh et al. 2015; Li et al. 2015), but there is disagreement as to whether there are other particle-specific characteristics of AgNPs that cause toxicity (Behra et al. 2013; Khan et al. 2015; Hu et al. 2018). Some argue that Ag^{+} is the only toxic component of the AgNPs to a variety of organisms (Xiu et al. 2012; Loza et al. 2014; Sakamoto et al. 2015; Shen et al. 2015), however, other studies have found evidence suggesting particle-specific toxic modes that also contribute to toxicity. These examples include observing inconsistencies between predicted versus actual Ag^{+} concentrations at AgNP LC50s (Navarro et al. 2008a; Fabrega et al. 2011; Ivask et al. 2014; Khan et al. 2015; Hu et al. 2018), different biochemical responses from exposure to AgNPs rather than Ag^{+} including different toxicogenomic responses (Poynton et al. 2012) or inhibited cellular Na^{+} uptake from AgNPs but not Ag^{+} (Schultz et al. 2012), and the exploration of different routes of exposure for AgNPs, such as

the uptake of entire AgNPs into cells or through ingestion, resulting in different levels of toxicity (Lee et al. 2007; Navarro et al. 2008b; Fabrega et al. 2011; Garcia-Alonso et al. 2011; Khan et al. 2015; Minghetti and Schirmer 2016; Conine and Frost 2017; Stevenson et al. 2017). Without a complete understanding of the different modes through which AgNPs induce toxicity, their environmental toxicity or bioavailability cannot be accurately evaluated.

Improving AgNP toxicity understanding has proven to be challenging for a number of reasons. First, AgNPs are extremely sensitive to their surrounding environments. Temperature, pH, dissolved oxygen, dissolved organic matter, and freshwater ion composition all affect the physical and chemical behaviors of AgNPs (Gao et al. 2009; McLaughlin and Bonzongo 2012; Unrine et al. 2012; Cupi et al. 2016; Conine et al. 2017). An important behavior for toxicity is the dissolution of Ag^+ from the AgNP surface, which simultaneously increases the Ag^+ concentration in solution and reduces the size of the AgNPs (Behra et al. 2013; Merrifield et al. 2017). Other behaviors include the aggregation of colliding AgNPs (Li et al. 2010; Huynh and Chen 2011; Chen and Zhang 2014), or sedimentation of AgNPs and their heavier aggregates out of a water column (Stebounova et al. 2011; Baalousha et al. 2013; Furtado et al. 2014; Ellis et al. 2018). Aggregated AgNPs have reduced surface area from which Ag^+ can dissolve, and multiple studies have confirmed reduced Ag^+ concentration in solutions with heavily aggregated particles (Zhang et al. 2011; Li and Lenhart 2012; Yue et al. 2015). Sedimentation rates are connected to the aggregation of AgNPs because larger aggregates sink more rapidly in solution than smaller aggregates or single particles. This process can severely alter the environmental transportation of AgNPs, and also decrease their concentration in the water column.

Sedimentation may reduce AgNP bioavailability to organisms that live in the water column, but may instead increase AgNP exposure to benthic organisms (Mclaughlin and Bonzongo 2012; Baalousha et al. 2013; Behra et al. 2013; Römer et al. 2013; Schultz et al. 2014).

The second challenge to studying the toxicity of AgNPs is that they exist with a myriad of different physical characteristics such as different particle sizes, capping agents, particle synthesis methods, or particle ages. AgNPs with different combinations of characteristics often elicit different levels of toxicity or different physical and chemical behaviors. For example, AgNPs can be synthesized across the entire 1 – 100 nm nanoparticle definition and size has been shown to be a significant determining factor of toxicity. Smaller AgNPs are regularly more toxic than larger AgNPs to a variety of organisms including bacteria, algae, crustaceans, and mammalian cells (Beer et al. 2010; Römer et al. 2013; Ivask et al. 2014; Kennedy et al. 2015; Cupi et al. 2016). As another example, most AgNPs are covered in a capping agent, which helps them repel one another and remain in suspension as individual particles. Citrate or polyvinylpyrrolidone (PVP) are two commonly used capping agents, however, many other chemicals are used for this role, and identically sized AgNPs with different capping agents can behave differently and have different toxicities (El Badawy et al. 2010; Kennedy et al. 2010; Asghari et al. 2012; Tejamaya et al. 2012; Pokhrel et al. 2013; Jimenez-Lamana and Slaveykova 2016). Kittler et al. (2010) showed that the concentration of Ag^+ in synthesized AgNP stock solutions with different capping agents increases at a first order reaction rate and can rapidly increase after several days of storage. Using AgNPs that are not newly synthesized will likely falsely increase AgNP toxicity due to excess Ag^+ and using AgNPs of inconsistent storage times likely adds an uncontrolled factor that affects toxicity. Finally, the selected method of AgNP

synthesis may affect the toxic properties of AgNPs (Fabrega et al. 2011; Behra et al. 2013). AgNPs are typically synthesized using "bottom up" reactions that turn silver salts into solid particles and can be formed from a variety of silver salts, solvents, and reducing agents, even if the capping agent remains consistent (Tolaymat et al. 2010). Beyond materials, different practices may include filtering or intentionally aging AgNP solutions, using different ratios of reducing agents to salts, or centrifuging stock solutions (Pillai and Kamat 2004; Kennedy et al. 2010; Croteau et al. 2014; Park et al. 2014). With so many different kinds of AgNPs used in toxicity testing, and each characteristic able to influence toxicity, there is limited consensus on what the overall toxicity of AgNPs is, or why these different characteristics affect the toxicity.

Without considering toxicity, some AgNP behaviors are extremely predictable, particularly in testing conditions with very few variables. AgNPs have been proven to behave according to the Derjaguin-Landau-Verwey-Overbeek (DLVO) theory of colloidal stability, which describes how cation concentrations predictably increase the aggregation rates of a colloid (Chen and Elimelech 2006; Huynh and Chen 2011; Stebounova et al. 2011; Baalousha et al. 2013; He et al. 2013; Chen and Zhang 2014). Briefly, AgNPs are small enough that, like many colloids, they have a negatively charged electric double layer (EDL). This EDL is strong enough that particles repel one another when they collide and consequently remain suspended as individual single nanoparticles. When attractive forces acting on the particle, such as van der Waals intermolecular forces, exceed the repulsive force of the EDL, a "successful collision" occurs, where colliding particles stick to one another to form an aggregate (two or more adhered AgNPs). Enough cation presence in solution can effectively reduce the state of the EDL to varying degrees, which reduces the

strength of attractive force necessary for successful collisions. The metric for the reduced state of the EDL is called the attachment efficiency (α), which is the measurable ratio of the aggregation rate at a particular salt concentration to the aggregation rate where 100% of collisions are successful. Increased valency of the cation significantly increases attachment efficiency, for example, Al^{3+} is more efficient than Ca^{2+}, which is more efficient than Na^{+} (Huynh and Chen 2011; Baalousha et al. 2013; Chen and Zhang 2014). Since aggregation rate is dependent upon the collision frequency, the concentration of particles/mL also plays a role in aggregation rates by affecting collision frequency (Piccapietra et al. 2012; Baalousha et al. 2013; He et al. 2013; Kim et al. 2017; McGillicuddy et al. 2017).

Depending on the water composition, the concentrations of different anions can also change how AgNPs behave. Chloride is a very reactive anion with AgNPs because of how easily AgCl can precipitate. This precipitation occurs directly onto the surface of the AgNP (Ameer et al. 2014; Chambers et al. 2014; Zook et al. 2014), which acts as a bridging mechanism that promotes the aggregation of colliding particles (El Badawy et al. 2010; Li et al. 2010; Baalousha et al. 2013). AgCl precipitation also occurs in solution with Ag^{+} that has dissolved from the AgNP, reducing the bioavailability of that Ag^{+} and therefore that component of AgNP toxicity (Di Toro et al. 2001; Groh et al. 2015; Yue et al. 2015; Gonçalves et al. 2017). When enough AgCl precipitates in solution, small AgCl nanoparticles (AgCl-NPs) form. While these nanoparticles still decrease the bioavailability of Ag^{+} to aquatic organisms, this process increases the overall nanoparticle concentration in solution (Peterson et al. 2015; Kim et al. 2017; Merrifield et al. 2017).

The effects of other anions like SO_4^{2-} or NO_3^{-} are less explored than Cl^{-}. The effects are usually only explained in comparison to Cl^{-} and can change depending on the properties

of both the AgNPs and the cations that they are paired with. Baalousha et al. (2013), using 30 nm AgNPs, found $\alpha_{NaCl} > \alpha_{NaNO_3} > \alpha_{Na_2SO_4}$. The authors explained the differences as the SO_4^{2-} and NO_3^- lacking the precipitating abilities of Cl^-. When the authors paired the same anions with Ca^{2+} instead of Na^+, however, there was little difference between the attachment efficiencies of the Ca^{2+} salts, indicating that the electric shielding abilities of Ca^{2+} overwhelmed the influence of each anion. Gebauer and Treuel (2011) paired the same anions with K^+ and, using 50 nm AgNPs, found $\alpha_{K_2SO_4} > \alpha_{KCl} > \alpha_{KNO_3}$, in disagreement to the anion order that Baalousha et al. (2013) found for monovalent Na^+ salts. Li et al. (2010), using 80 nm AgNPs, disagreed with the anion conclusions of both studies and concluded that $\alpha_{NaNO_3} > \alpha_{NaCl}$. These inconsistent and limited findings not only reveal a gap in understanding but also indicate that attributing all AgNP chemical behaviors to the properties of environmental cations may be an incomplete approach, particularly if anions like Cl^- elicit an effect with some cations but not all. Many studies on AgNP kinetics have compared the aggregating abilities of different cations by using chloride salts. This practice ignores that Cl^- ratios double or triple in tests with higher valency cations (e.g. Chen and Elimelech 2006; Li et al. 2010; Huynh and Chen 2011; Liu et al. 2011; Chen and Zhang 2014), and also that Cl^- has been shown to increase the aggregating effects of monovalent but not di- or trivalent cations (Baalousha et al. 2013). Furthermore, the sensitivity of AgNPs to electrolyte chemistry but limited information on anion effects indicates that substituting Cl^- with a different anion in toxicity testing solutions (e.g. Yue et al. 2015) may be testing the effect of the substituted anion rather than simply the removal of the Cl^-.

These experiments to measure kinetic behavior occurred in very controlled environments with solutions composed of just deionized distilled water and one, or

occasionally two, salts present at high concentrations (Chen and Elimelech 2006; El Badawy et al. 2010; Li et al. 2010; Gebauer and Treuel 2011; Huynh and Chen 2011; Liu et al. 2011; Baalousha et al. 2013; Chen and Zhang 2014; Kim et al. 2017). Toxicity testing conditions, however, are first designed around the survival needs of the organism, which require more complex solutions composed of multiple salts at lower concentrations, dissolved oxygen, specified pH or alkalinity, and occasionally food (OECD 2004; ISO 2012; ASTM 2012; ASTM 2014), so the particle behavior reported in kinetic studies does not reflect how particles behave in toxicity testing conditions. Furthermore, typical AgNP concentrations that produce concentration-response curves for a range of organisms (Lee et al. 2007; Asghari et al. 2012; Gottschalk et al. 2013; Groh et al. 2015; Goncalves et al. 2017) are much lower than those used in studies focused on kinetic behavior (e.g. El Badawy et al. 2010; Stebounova et al. 2011; Baalousha et al. 2013; Chen and Zhang et al. 2014). Aggregation rates, influenced by particle concentration, will be affected by a lower collision rate and will not necessarily remain constant across increasing concentrations of a toxicity test (Piccapietra et al. 2012; Kim et al. 2017).

The number and type of variables present in toxicity testing conditions are often unavoidable and add additional factors that affect AgNP behavior. The extreme sensitivity of AgNPs and other ENMs to their surrounding environment has led researchers to advocate for improved standardized methods specifically for nanomaterial testing (e.g. Kennedy et al. 2015; Peterson et al. 2015; Cupi et al. 2016; Merrifield et al. 2017). ASTM International (ASTM), the Organization for Economic Co-operation and Development (OECD), and the International Organization for Standardization (ISO) each have their own requirements for reconstituted freshwater used for *Daphnia magna* acute toxicity tests.

ASTM is the most stringent, requiring that their recipe of four salts ($NaHCO_3$, $CaSO_4$, $MgSO_4$, and KCl) be used unless unfeasible for the experiment (ASTM 2014). The ISO method offers a recipe that is composed of the same four salts as the ASTM method but with $CaCl_2$ substituted for $CaSO_4$, however the ISO method also clarifies that any freshwater is allowed as long as it is compliant with the water quality criteria outlined in the document (ISO 2012). The OECD method is similar to the ISO method in that it provides the water quality criteria and allows any freshwater that is in accordance with them (OECD 2004). OECD provides the ISO recipe as an option, followed by two additional recipes for freshwaters known as Elendt M4 and M7, which each have more than a dozen ingredients. Although M4 and M7 are not recommended for tests using metals, they are occasionally used in AgNP toxicity tests (Lee et al. 2012; Park et al. 2014), sometimes with the metal chelating agent removed (e.g. Khan et al. 2015). Similarly complex recipes are also used and are still in accordance with OECD guidelines (Sakamoto et al. 2015). The differences in electrolyte composition between standardized recipes and guidelines makes it unsurprising that AgNP toxicity differs depending on the selected method (Cupi et al. 2017; Hu et al. 2018; Kidd et al. 2018).

Furthermore, the recommended water quality for test solutions in each standardized method are too broad to produce consistent AgNP toxicity results. Both ISO and OECD recommend—rather than require—that waters have a pH between 6 and 9, and a hardness between 140 – 250 mg/L $CaCO_3$. This pH range induces different rates of Ag^+ dissolution from the AgNP surface, which causes changes in dissolved Ag^+ concentrations and different levels of toxicity (Liu and Hurt 2010; Seitz et al. 2015; Molleman and Hiemstra 2017). An increase in water hardness from 140 to 250 mg/L $CaCO_3$ almost

doubles the Ca^{2+} concentration from 56 – 100 mg/L. This difference in divalent cation concentration should have significantly different aggregation effects on AgNPs (Cupi et al. 2016), which is a behavior that affects the dissolution of aqueous Ag^{+} from the AgNPs (Zhang et al. 2011; Li and Lenhart 2012; Schultz et al. 2014; Yue et al. 2015). Since usually only the selected standard toxicity method and recipe are reported rather than precise and measured water quality conditions, the results of reported AgNP toxicity tests can have limited interpretation—or be misinterpreted—and can be challenging to reproduce (Groh et al. 2015; Peterson et al. 2015).

In addition to improving the precision of testing conditions, the metric of measuring AgNP toxicity as a mass of Ag is being voiced as inappropriate for characterizing toxicity test results (Hull et al. 2012; Merrifield et al. 2017). The assumption in toxicology is that mass or molar units quantify the potency of a toxicant, however this description does not apply to AgNPs (and other ENMs) because so much of the mass of AgNPs is stored in the interior of the particle, where it does not react or interact with the surrounding environment. Additionally, Hull et al. (2012) points out that the same mass can describe either few large particles or many smaller particles, which reflect different particle concentrations and particle surface areas that are available to interact with the environment or from which Ag^{+} can dissolve. Particle concentration, particle surface area, or just the dissolved Ag^{+} concentration in solution are other dose metrics being considered to describe AgNP toxicity, as they are considered better descriptors of what causes toxicity (Kennedy et al. 2015; Peterson et al. 2015; Merrifield et al. 2017).

The purpose of this study was to understand the impacts that the freshwater ions Ca^{2+}, Na^{+}, Cl^{-}, and SO_4^{2-} have on AgNP toxicity and chemical behavior in ASTM acute

D. magna toxicity testing conditions. Observing how manipulated concentrations of these ions in a standardized recipe affect AgNP toxicity, particle size, particle sedimentation, and particle concentration could improve understanding on the specific way that AgNPs behave in standardized toxicity tests, and how particular differences between recipes may change the toxicity results. These findings could inform methods for standardization and potentially connect specific particle behaviors to differences in toxicity.

Methods

Experiment Design

A factorial experiment design based on salts was utilized to create different treatments of toxicological media. Moderately hard synthetic freshwater (MHW) (USEPA 2002), which consists of 0.348 mM $CaSO_4$, 0.498 mM $MgSO_4$, 0.054 mM KCl, and 1.14 mM $NaHCO_3$, was used as the baseline recipe. Experimental freshwaters were created by adding three salt treatments in a factorial design to the MHW baseline recipe: 0.856 mM NaCl, 0.427 mM $CaCl_2$, and 0.428 mM Na_2SO_4 (Table 1). Toxicity tests and AgNP chemical behavior measurements were conducted in each experimental freshwater.

While the goal of this study was to investigate the effects of specific ions rather than salts, the factorial experiment design is only able to make statements about the salt treatments as cation/anion pairs. A factorial design based on ions cannot be used because adding a particular ion to solution necessitates the addition of a counter ion; increasing the level of one ion as a factor will always increase the level of a second ion, so effects cannot be isolated to either ion, and, more importantly, become collinear factors. To overcome some of these obstacles, the fixed concentrations of each salt factor in this study were

selected such that the dissociated ion concentrations from different salt treatments were equivalent (Table 2). For example, any difference observed between results from the water with just the NaCl treatment (NC) and the water with just the Na_2SO_4 treatment (NS) can be attributed to the effect of the substituted anion because the Na^+ concentration in both waters was the same. The NaCl and $CaCl_2$ treatments added the same Cl^- concentration therefore differences between the effects of these salts were due to the difference in cation. This design allows for discussion about the effects of individual ions, however, the factorial analysis may only determine the effects of an entire salt treatment composed of both added ions. Table 3 shows the total concentration of each ion in each experimental water resulting from the baseline MHW recipe and the added salt treatment.

Table 1. Factorial experiment design indicating the presence (+) or absence (-) of the three salt treatments added to a MHW baseline to create each experimental freshwater. Each water is named according to its salt treatment: NaCl becomes NC, $CaCl_2$ becomes CC, and Na_2SO_4 becomes NS.

	NaCl	$CaCl_2$	Na_2SO_4	Water name
Water 1	-	-	-	MHW
Water 2	-	-	+	NS
Water 3	-	+	-	CC
Water 4	-	+	+	CC-NS
Water 5	+	-	-	NC
Water 6	+	-	+	NC-NS
Water 7	+	+	-	NC-CC
Water 8	+	+	+	NC-CC-NS

Table 2. Concentrations of individual dissociated ions added to experimental freshwaters from each salt treatment.

	Concentration added to freshwaters (mM)				
Addition salt	Salt concentration added	Na^+	Ca^{2+}	Cl^-	SO_4^{2-}
NaCl	0.856	0.856	-	0.856	-
$CaCl_2$	0.427	-	0.427	0.853	-
Na_2SO_4	0.428	0.855	-	-	0.428

Table 3. Total concentrations (MHW baseline plus salt treatment) of each ion present in each experimental freshwater, as well as total ionic strength. Each freshwater also contains uniform nominal concentrations of K (0.054 mM), Mg (0.498 mM), and HCO_3 (1.14 mM) that are present in the baseline MHW recipe.

	Total Concentration (mM)				
Test Water	Na^+	Ca^{2+}	Cl^-	SO_4^{2-}	Ionic Strength
MHW	1.14	0.348	0.054	0.847	9.17
NS	2.00	0.348	0.054	1.275	11.73
CC	1.14	0.775	0.907	0.847	11.73
CC-NS	2.00	0.775	0.907	1.275	14.29
NC	2.00	0.348	0.909	0.847	10.88
NC-NS	2.85	0.348	0.909	1.275	13.44
NC-CC	2.00	0.775	1.763	0.847	13.44
NC-CC-NS	2.85	0.775	1.763	1.275	16.01

Factorial analysis on salts was performed following Berthouex and Brown (1994) and NIST/SEMATECH (2012) to determine whether the NaCl, $CaCl_2$, or Na_2SO_4 salt treatments, or any interactions between them had significant effects on AgNP toxicity or behavior. If analyzed endpoints did not have replication (and therefore not enough degrees of freedom to test all factors and interactions), a two-directional stepwise regression based on AIC was employed to determine significant model terms (NIST/SEMATECH 5.4.7.1. 2012). These terms were confirmed by plotting factor and interaction effects against normal order scores to observe whether selected effects or interactions did not follow the pattern of a random distribution (NIST/SEMATECH 5.5.9.8. 2012).

Biotic Ligand Model

The Biotic Ligand Model was run for Ag^+ using Windward Environmental, LLC's (Seattle, WA) Biotic Ligand Model Software (*Biotic Ligand Model*, version 3.36.2.45, 2018). Nominal concentrations for each freshwater ion were input for each experimental water as

well as the water quality conditions of the toxicity tests (Table 4). Water quality conditions were entered as uniform values across all waters. Temperature, pH, and alkalinity were measured during toxicity testing and the averaged values were used for model inputs. DOC, NO_3, and S were not present in the experimental waters but the BLM recommends inputting the value 1.0×10^{-10} mg/L rather than 0. The BLM assesses humic acid as a percentage of DOC and recommends 10%, rather than 0%, as the lowest input value. Output for the model included predicted Ag^+ LC50s for each experimental water, as well as the partitioning of Ag and its species at predicted LC50 concentrations. Factorial analysis was performed on the BLM-predicted Ag^+ LC50s for each experimental water.

Table 4. Water quality conditions as inputs to the BLM based on toxicity testing conditions.

Temperature (°C)	20
pH	8
DOC (mg-C/L)	1.0×10^{-10}
Humic acid (%)	10
NO_3 (mg/L)	1.0×10^{-10}
Alkalinity (mg/L $CaCO_3$)	61.04
S (mg/L)	1.0×10^{-10}

AgNP Synthesis

Citrate-capped AgNPs were synthesized according to Lee and Meisel (1982). Briefly, $AgNO_3$ was boiled with 1% sodium citrate solution for exactly one hour. To reduce variation between batches, production variables were kept as consistent as possible during each synthesis (Table 5). The nominal concentration of the synthesized stock solutions was 116.2 mg/L (total Ag). Different batches of AgNPs were used throughout the analytical and toxicity tests. All analytical or toxicity tests used AgNPs within 24 hours of synthesis to create more consistency in the concentration of Ag^+ that may have dissolved into solution

and to reduce variation of Ag^+ concentrations between batches (Kittler et al. 2010). Despite this effort to minimize the age of the AgNPs, it is still possible that there were differences in batches. To account for impacts caused by different AgNP batches on particle and toxicity measurements, batch was included in ANOVAs as a random factor and the F statistics of the factors of interest were therefore calculated using the expected mean square from batch.

Table 5. Materials and conditions used for AgNP synthesis.

$AgNO_3$	18.3 mg
1% sodium citrate solution	2.00 mL
Temperature	390 – 415°C
Stir rate	330 rpm
Batch Volume	100 mL
Glassware	150 mL beaker
Water replacement	~1.5 mL / min

Toxicity Tests and statistical analysis

Acute toxicity tests (ASTM 2014) were performed twice in each experimental freshwater using *D. magna* neonates. For each toxicity test, six AgNP concentrations and a negative control were triplicated in glass test chambers, using five organisms per chamber. Mortality was counted at 24 and 48 hours. Organisms were purchased from *Aquatic BioSystems, Inc.* (Fort Collins, CO). Tests were performed at 20.0°C in a 16:8 hour light:dark cycle.

AgNPs were added from the stock solution to each individual test chamber already filled with experimental freshwaters and gently pipette mixed before neonates were added. By adding AgNPs directly to each test chamber all physical and chemical behaviors that occurred as a result of the AgNPs interacting with the salt treatments, occurred within the

test chamber. All chambers received AgNPs before any neonates were added to any chambers. Organisms were added anywhere from 1 to 35 minutes after the AgNPs were added to the chambers.

Concentration-response curves and point estimates for each experimental water were calculated from the combined mortality counts from both toxicity tests on R statistical software (R Core Team 2017) using the 3-parameter log-logistic model in the drc package (Ritz et al. 2015). Statistical comparisons between point estimates of different waters were made by comparing ratio parameters using the compParm function in the same package. A two-factor factorial analysis was performed on the LC50s of the four experimental waters without Na_2SO_4 (MHW, NC, CC, NC-CC; Table 1) to test the main effects and interactions between NaCl and $CaCl_2$ on AgNP toxicity.

UV-Vis

Sedimentation of AgNPs in each experimental water was measured using a UV-Vis spectrophotometer (8542 Diode-Array Spectrophotometer, Hewlett Packard, CA) paired with a chiller to maintain the temperature of the samples at 20.0°C throughout the duration of the test. AgNPs were added to each experimental water with no added *D. magna* in 10 mm plastic cuvettes at a concentration of 10 mg/L, which trial runs showed resulted in clear and consistent initial peak absorbances. Sedimentation experiments in each water were replicated five times. AgNPs were pipette-mixed to evenly distribute throughout the cuvette, and absorbance measurements began less than 10 seconds after mixing. During trial runs, peak absorbance in the broad spectra was observed to be $\lambda = 416 \pm 4$ nm, which is consistent with other findings in the literature (Bhui et al. 2009; Stebounova et al. 2011;

Asghari et al. 2012; Ivask et al. 2014); absorbance measurements over time were therefore taken at λ = 416 nm. Measurements were taken at an interval of 36.6 sec for 3.5 hrs after AgNP addition, which trial runs showed captured the immediate initial aggregation that rapidly removed AgNPs from the water column as well as some time with much slower rates of particle removal as absorbances approached a plateau. UV-Vis measurements were carried out by WWU undergraduate Winston Booth.

Rate analysis was performed on the absorbance readings over time using Graphpad Prism software (Graphpad Software 2017). The best fit model for all waters was found to be a three-phase decay model based on AIC, which the software fit to each experimental water from that water's five replicates. Subsequent factorial analyses were performed on the fast, medium, and slow rate constants (k_{fast}, k_{medium}, and k_{slow}) as well as the predicted plateaus from the models that were fit to each experimental water.

A repeated measures ANOVA was performed on absorbance readings for each water at time (T) = 0 min, 8 min, 15 min, 30 min, 1 hr, 2 hr, and 3.5 hr to test whether experimental water had a significant impact on how absorbance changed over time (α = 0.05). Simple main effects contrasts were performed following significant interactions between water and time comparing the differences between waters at each time (family α = 0.05). Synthesized AgNP batch was included as a random factor in two-way ANOVAs of absorbance readings at each time.

ICP-MS

Particle size and particle concentration were measured on ICP-MS (Agilent 7500ce, Agilent Technologies, CA) using the single particle inductively coupled plasma mass

spectrometry (spICP-MS) technique originally described in a series of papers by Degueldre et al. (i.e. Degueldre and Favarger 2003, 2004; Degueldre et al. 2004, 2006a, 2006b). Transport efficiency was calculated using the Particle Size Method according to Pace et al. (2011), using standardized 60 nm gold nanoparticles (U.S. National Institute of Standards and Technology, RM 8013) and corresponding dissolved gold standards. Transport efficiency was measured on each day of testing and ranged from 3.01 – 6.15%.

AgNP samples for ICP-MS analysis were prepared as in the toxicity tests with glass test tubes and pipette mixing AgNP LC50 concentrations ± 14% (Table 6) into each corresponding experimental freshwater. Aliquots for ICP-MS analysis were sampled from the middle of the water column in each test tube. Measurements of Ag^{107} were taken 3.5 hours and 24 hours after AgNPs were added to observe changes in particle measurements during the time when the most mortality occurred based on qualitative observations. Replicates of each experimental freshwater at each time were independent (not repeated measurements). Three 60-sec measurements were taken per sample replicate at each measurement. The instrument was limited to a minimum of 10 ms dwell times therefore samples were diluted in deionized distilled water to a concentration resulting in 5.00 ± 1.47% particle event readings in each 60-sec sample measurement. This is recommended to avoid coincidences, where multiple particles are measured during a single dwell time thereby falsely increasing particle size measurement and reducing particle concentration (Montano et al. 2014, 2016).

AgNP measurements, referred to as events, were separated from background readings by treating all dwell time measurements $\mu + 5\sigma$ (where μ and σ are mean and standard deviation, respectively) as particles. Particle events that surpassed 5σ above the

mean were removed from the dataset and the threshold was applied again (Bi et al. 2014; Montano et al. 2016; Miyashita et al. 2017). Events were classified this way until no more values existed above the threshold. Coincidences were removed as outliers using Grubbs' test by testing separated events from each 60-second sample measurement on Graphpad Outlier Calculator ($\alpha = 0.01$) (Graphpad Software 2018). Due to the monodisperse nature of the standardized gold nanoparticles paired with little to no dissolved gold background, particle events for gold nanoparticles were separated from background readings using the K-means clustering method described in Bi et al. (2014).

Table 6. Percent differences between calculated LC50s from toxicity testing results and nominal AgNP concentrations used for ICP-MS measurements in each experimental water.

Experimental Water	Calculated LC50 from toxicity testing (μg/L)	Nominal AgNP concentration for ICP-MS (μg/L)	Percent Difference
MHW	53.48	52.29	2.23
CC-NS	84.20	84.25	-0.06
NC	97.75	98.77	-1.04
CC	118.69	118.52	0.14
NC-NS	217.16	214.97	1.01
NC-CC	383.52	331.17	13.65

Particle size distribution and particle concentration were calculated according to Pace et al. (2011, 2012). Due to the presence of multiple distributions in the resulting size histograms, samples were divided into three size categories: < 60 nm, 60 – 100 nm, and > 100 nm. 60 nm was selected because reformed AgNPs or AgCl-NPs and the majority of their aggregates are likely to be represented in entirety in this size category (Baalousha et al. 2013; Kim et al. 2017; Merrifield et al. 2017). The second category captures the

remainder of the original particles (treated as 71.55 ± 2.97 nm from preliminary measurements on DLS), including whether dissolution had reduced their diameter, and includes two- to three-particle aggregates (Kim et al. 2017). Particles greater than 100 nm indicate the occurrence of aggregates composed of more than four AgNPs (Montano et al. 2014; Kim et al. 2017). X^2 tests for independence were used to determine whether the electrolyte composition or duration of exposure between experimental waters affected the number of particles in each size category. Multiple X^2 tests were run to compare different sample types against one another and because some comparisons were isolated by AgNP batch. A Bonferroni correction was therefore applied to the X^2 statistic. When that statistic was significant, standardized residuals were calculated in a X^2 contingency analysis to determine where significant differences existed between expected and observed particles in each size category. Kolmogerov-Smirnov tests with a Bonferroni correction were performed on replicate samples to determine whether replicates had the same distributions. All replicate pairs except the NS water at 24 hrs found no difference between distributions so the number of particles in each size category of replicate pairs were averaged together and those averages were used in the X^2 tests for independence for those sample types. Despite being found to be from different distributions, the replicate pair of the NS water at 24 hrs was also averaged because there was no experimental reason to doubt the validity of either replicate.

The three 60-second measurements taken for each sample yielded three particle concentration measurements per replicate. Experimental water and duration of exposure were compared using two-way ANOVAs ($\alpha = 0.05$) that compared samples that were isolated by AgNP batch. A two-way ANOVA was also run to compare experimental water

and duration of exposure using all samples from all three AgNP batches with the understanding that batch may have affected particle concentration measurements. Following a nonsignificant interaction between water and time, pairwise t-tests were used to compare experimental waters. Pearson correlation tests were run comparing the particle concentrations at each time individually and as a combined range of both times against the respective LC50s of Ag by mass.

Results

A summary of statistical tests and outcomes performed on all AgNP and toxicity endpoints can be found in Table 7. The statistical tests and outcomes used to evaluate the effects of AgNP batch on each toxicity and instrument endpoint can be found in Table 8.

AgNP Batch

This study was not designed to test the effects caused by different AgNP batches, however, concerns were raised that AgNP batch may have had effects on particle behavior because the shapes of the particle size distributions from the ICP-MS appeared to be different depending on the batch used. For example, the MHW and NC size distributions at 3.5 hrs (from one batch) appear more similar to each other than the MHW and NC size distributions at 24 hrs (from a different batch), which were also very similar in appearance to one another (Figure 1). The remaining size distributions were all from a third batch and appear the most similar to each other regardless of difference in salt treatments or measurement times, and do not look the same as the size distributions from the other two batches. Due to this appearance of very different distribution shapes based on batch

(Figure 1), AgNP batch was incorporated into statistical tests as a precaution. To test batch effects, AgNP batch was incorporated post-hoc into the analyses of the particle characterization and toxicity measurements. The experimental designs for the tests performed in this thesis were able to accommodate the post hoc inclusions except for the experiments performed on ICP-MS, where the tested factors were nested entirely within AgNP batch. Since the effect of batch on particle size distribution appeared to dictate the number of particles in each particle size category and also possibly the size of the particles themselves (and therefore the locations of the distributions along the x-axis), it was concluded that the ICP-MS was likely able to determine significant effects of particle batch on particle size distribution. Regrettably, since tested factors (salt treatment and time) were nested within particle batches on ICP-MS measurements, the effect that batch had on particle size distributions could not be accounted for. There is no evidence from the literature that different batches from the same AgNP synthesis method do or do not influence particle measurements, however any significant effects on the particle sizes or the particle size distribution shape could have affected the X^2 independence and contingency analyses, which specifically compared the number of particles in each size categories between multiple samples. Therefore, statistical tests on ICP-MS particle size measurements were only considered statistically valid between measurements derived from the same synthesized AgNP batch. The use of multiple AgNP batches was not found to significantly affect the results of the toxicity tests or the UV-Vis experiments (Table 8).

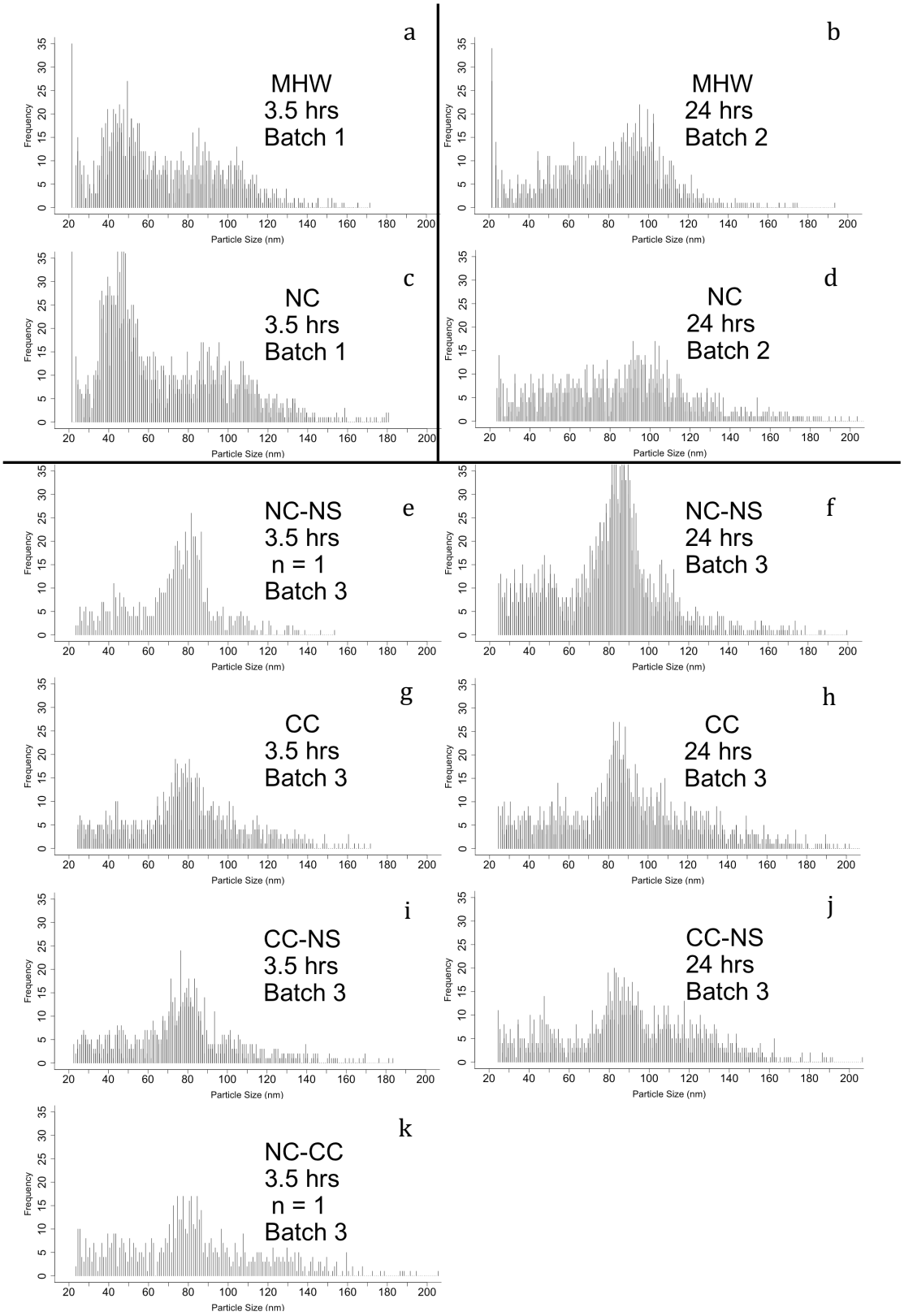

Figure 1. Particle size histograms (n = 2) of AgNPs measured using single particle ICP-MS. Experimental water, time of measurement, and AgNP batch are noted on each plot. Bolded lines isolate sample types by AgNP batch.

Table 7. Summary of statistical tests performed on measured and calculated endpoints.

Endpoint:	Tests Performed:	alpha correction?	Experimental waters compared:	Result:
Toxicity				
AgNP LC50	Ratio comparison test	none	MHW, NC, CC, NC-NS, CC-NS, NC-CC	CC-NS, NC, and CC were statistically similar to one another. All other LC50s were different from one another. All salt treatments reduced toxicity compared to MHW.
	Factorial analysis: NaCl, $CaCl_2$	none	MHW, NC, CC, NC-CC	NaCl, $CaCl_2$, and interaction of NaCl and $CaCl_2$ all significantly reduced AgNP LC50. (Na_2SO_4 not assessed)
BLM				
Model Output: Ag^+ LC50	Factorial analysis: NaCl, $CaCl_2$, Na_2SO_4	none	All waters	NaCl, $CaCl_2$, Na_2SO_4, and interaction of NaCl and $CaCl_2$ significantly increased predicted Ag^+ LC50.
UV-Vis				
Absorbance	Repeated measures ANOVA: diluted experimental water, 7 times of measurement	none	All waters	Experimental waters significantly changed absorbance over time. The waters did not change absorbance the same (therefore performed simple main effects contrasts).
	Simple main effects contrasts following significant water:time interactions on repeated measures ANOVA	Bonferroni	All waters	Experimental waters were different from one another up through 1 hr of test time, but after 2 hr, absorbances were no longer different between waters. Waters with $CaCl_2$ were always statistically similar and had low absorbances. MHW and NS were always statistically similar and had the highest absorbances (indicating slower sedimentation).

Endpoint:	Tests Performed:	alpha correction?	Experimental waters compared:	Result:
3-phase decay model components	Factorial analysis: NaCl, $CaCl_2$, Na_2SO_4	none	All waters	$CaCl_2$ significantly affected all three rate constants (k_{fast}, k_{medium}, and k_{slow}). NaCl affected the medium rate and likely the fast rate (but was barely nonsignificant). Na_2SO_4 was nonsignificant on all rate constants. Modeled plateau was unaffected by any salts.
ICP-MS				
Particle size distribution	Kolmogorov-Smirnov test between sample replicates	Bonferroni	MHW, NC, CC, NC-NS, CC-NS	Replicate samples came from the same distributions, except for NC-NS after 3.5 hrs (n = 1) and 24 hrs (different distributions).
	X^2 test for independence comparing particle distribution in 3 size categories	Bonferroni	Table 14; MHW, CC-NS, NC, CC, NC-NS, NC-CC	All tests described in Table 14 had significantly different distributions except for the difference between MHW and NC after 3.5 hrs, which showed no difference between the number of particles in each size category.
	X^2 contingency analysis following significant X^2 tests for independence	none	Table 14; Appendix B	Waters with $CaCl_2$ had more particles > 100 nm than waters without $CaCl_2$, which had more particles between 60 - 100 nm. Waters able to compare both measurement times found that there were more particles > 100 nm and fewer particles between 60 -100 nm after 24 hrs than at 3.5 hrs, indicating aggregation over time.
Particle concentration	Two-way ANOVA: experimental water, time spent in water	none	CC, CC-NS, NC-NS **(same batch)**	Experimental waters and duration of exposure both significantly affected particle concentration. The interaction between water and time was nonsignificant therefore exposure duration affected all three waters the same.

Endpoint:	Tests Performed:	alpha correction?	Experimental waters compared:	Result:
Particle Concentration	Two-way ANOVA: experimental water	none	MHW, NC (3.5 hrs) **(same batch)**	Particle concentrations between MHW and NC were different after 3.5 hrs.
	Two-way ANOVA: experimental water	none	MHW, NC (24 hrs) **(same batch)**	Particle concentrations between MHW and NC were the same after 24 hrs.
	Two-way ANOVA: experimental water, time spent in water	none	MHW, CC-NS, NC, CC, NC-NS, NC-CC **(different batches ignored)**	Experimental waters and duration of exposure both significantly affected particle concentration. The interaction between water and time was nonsignificant therefore exposure duration affected all waters the same.
	Pairwise t-tests comparing individual experimental waters	none	MHW, CC-NS, NC, CC, NC-NS, NC-CC **(different batches ignored)**	Despite LC50s from 53.48 – 118.69 µg/L, MHW, CC-NS, NC, and CC all had statistically similar particle concentrations. NC-NS and NC-CC had higher particle concentrations that were similar to one another, however NC-NS was missing data for one replicate.
	Pearson correlation test against LC50	none	MHW, CC-NS, NC, CC, NC-NS, NC-CC **(different batches irrelevant)**	Particle concentrations were positively correlated with LC50 at both 3.5 and 24 hrs.

Table 8. Analyses used to determine whether AgNP batch affected measured endpoints.

Test/ Instrument	Endpoint	# of batches used	Statistical Test(s) for batch significance	Test outcome	Implication for Results
Toxicity Tests	LC50	8	Two-way ANOVA testing experimental water and batch	Batch was nonsignificant	Toxicity results were not affected by variation from AgNP batch
UV-Vis	Absorbance at 15, 30, 60, and 210 min	Every water was represented by at least 3 different batches	Two-way ANOVAs testing experimental water and batch at each measurement time	Batch and the interaction between water and batch were nonsignificant at all times	All effects observed were due to the salt treatments. (Repeated measures ANOVA was not possible because not every water was represented by every batch)
ICP-MS	Particle Size and Particle Concentration	3	No tests were performed. Waters were nested inside batch therefore no test could be performed to rule out variation contributed by batch	Assumption that batch had an effect	Only samples measured from the same batch were considered statistically valid against one another.

Toxicity

Effects of Na_2SO_4 and any associated interactions could not be tested in factorial analysis because the NS and NC-CC-NS waters did not pass data quality objectives, including: control mortality greater than 20%, unrepeatable results where replicated toxicity tests produced concentration response curves with 95% CIs that did not overlap, or tests that resulted in no effects at all concentrations. Statistical conclusions about salt treatments on toxicity did not include these two waters (NS and NC-CC-NS; Tables 7, 9).

All salt additions to experimental freshwaters reduced toxicity in comparison to MHW (Figures 2, 3). A two-factor factorial analysis performed on the waters without Na_2SO_4 (MHW, NC, CC, NC-CC) found NaCl, $CaCl_2$, and an interaction effect between them to each significantly increase AgNP LC50 (Figures 3, 4a; Tables 9, A1). Ratio comparisons of LC50s found the CC-NS, NC, and CC freshwaters to be statistically similar. This group was less toxic than MHW, but more toxic than NC-NS and NC-CC (Figure 2). In all tests, more than 90% of mortality occurred in the first 24 hrs of the 48-hr test.

Table 9. Descriptive statistics for measured AgNP LC50s in all experimental waters except NS and NC-CC-NS. Significance from factorial analysis indicates whether a salt or interaction was significant (Y) or not (N). Factorial analysis on AgNP LC50 reflects 2-factor analysis comparing just two salts across four waters: MHW, NC, CC, and NC-CC.

	Descriptive Statistics				Significant in Factorial Analysis?		
	Mean	Median	Min	Max	NaCl	$CaCl_2$	NaCl:$CaCl_2$
AgNP LC50 (μg/L)	159.13	108.22	53.477	383.52	Y	Y	Y

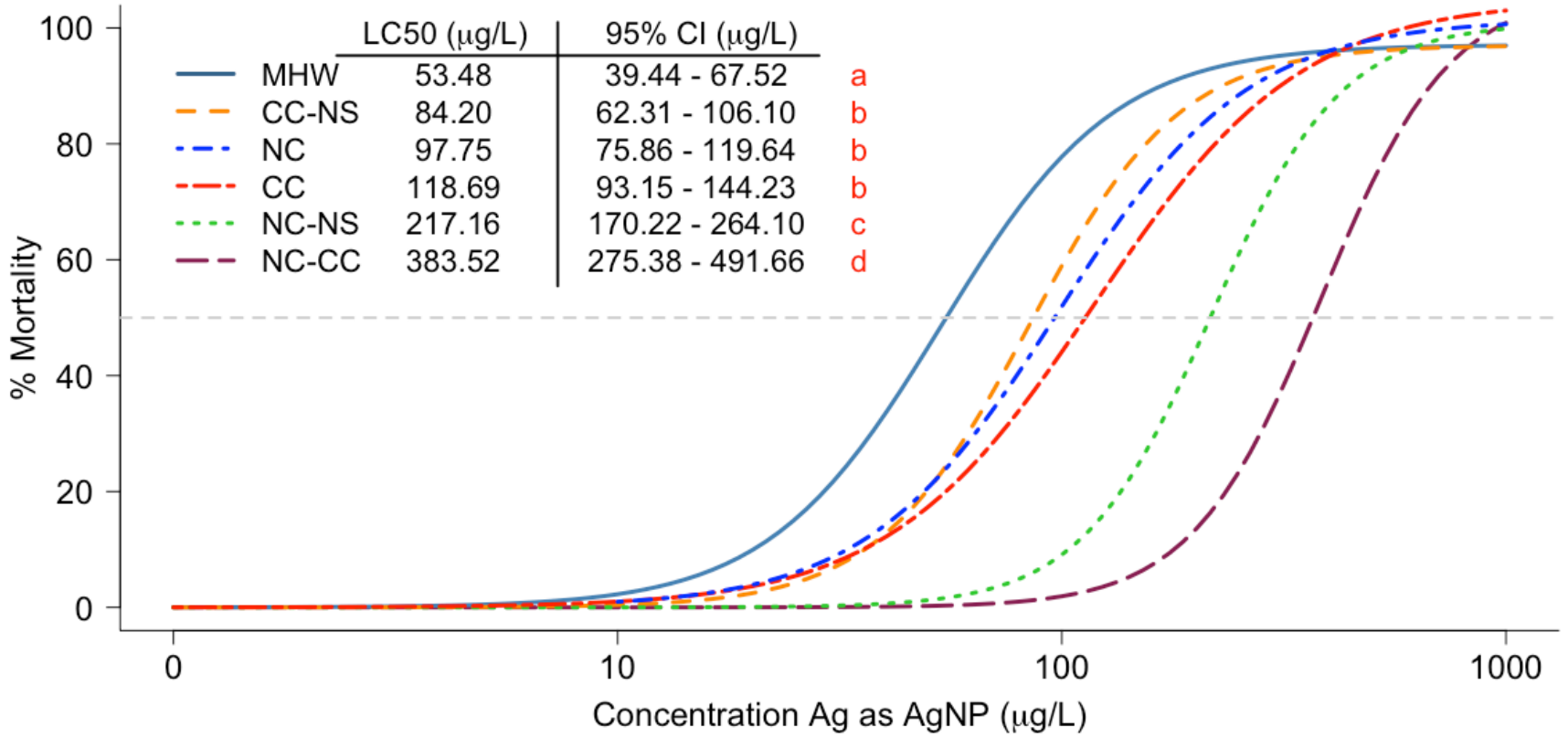

Figure 2. Acute concentration-response curves for AgNPs in six experimental waters modeled using a three-parameter log-logistic model. Letters show significant differences between LC50s, determined by ratio using the *compParm()* function of the drc package (Ritz et al. 2015).

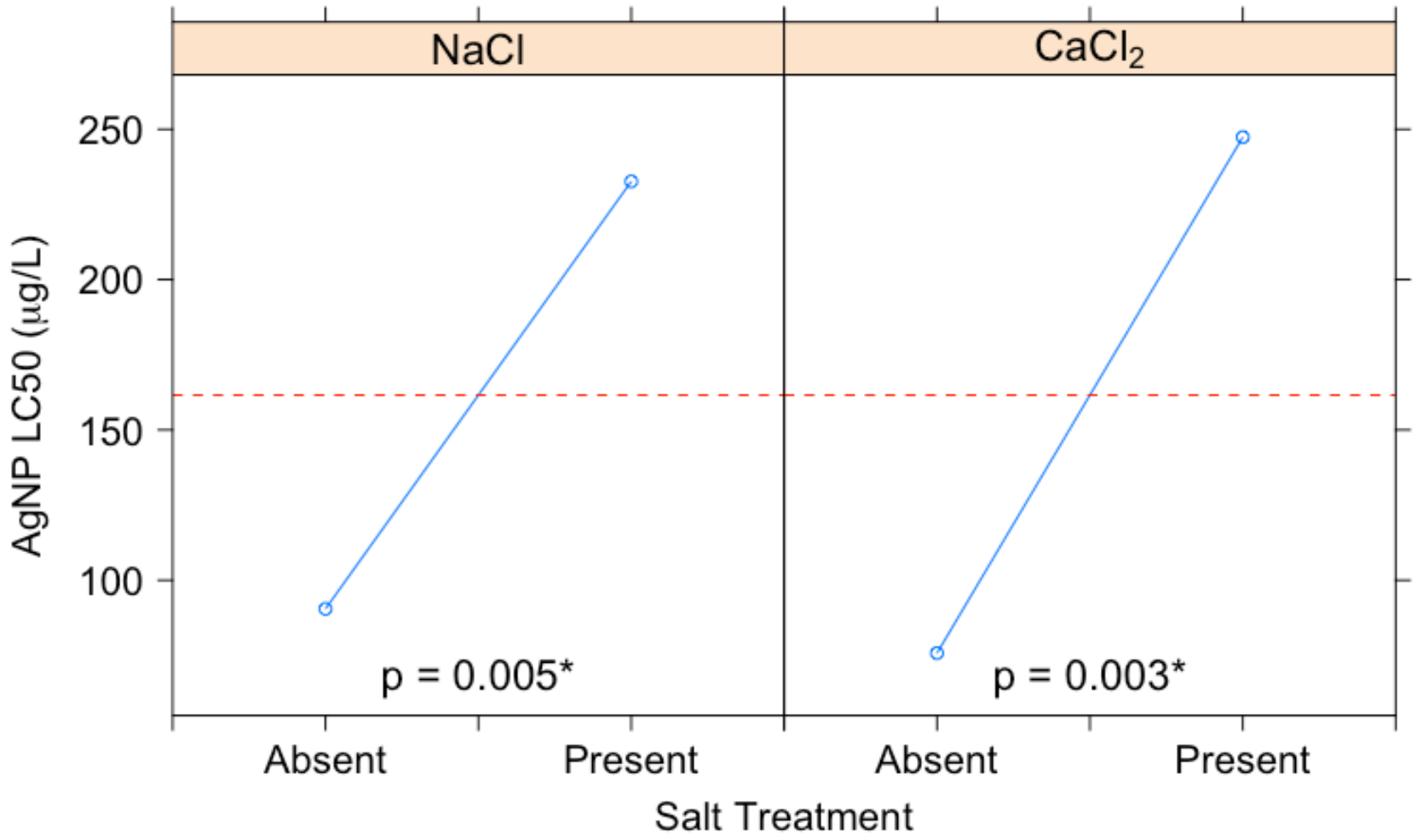

Figure 3. Main effects plots from the two-factor factorial analysis performed on the four waters without Na_2SO_4 (MHW, NC, CC, NC-CC) showing the effects of the addition of the NaCl and $CaCl_2$ salt treatments (present) on AgNP LC50 (n = 2) compared to the waters without each respective salt treatment (absent). The factorial model is in Table A1. Asterisks indicate the salt factor was significant.

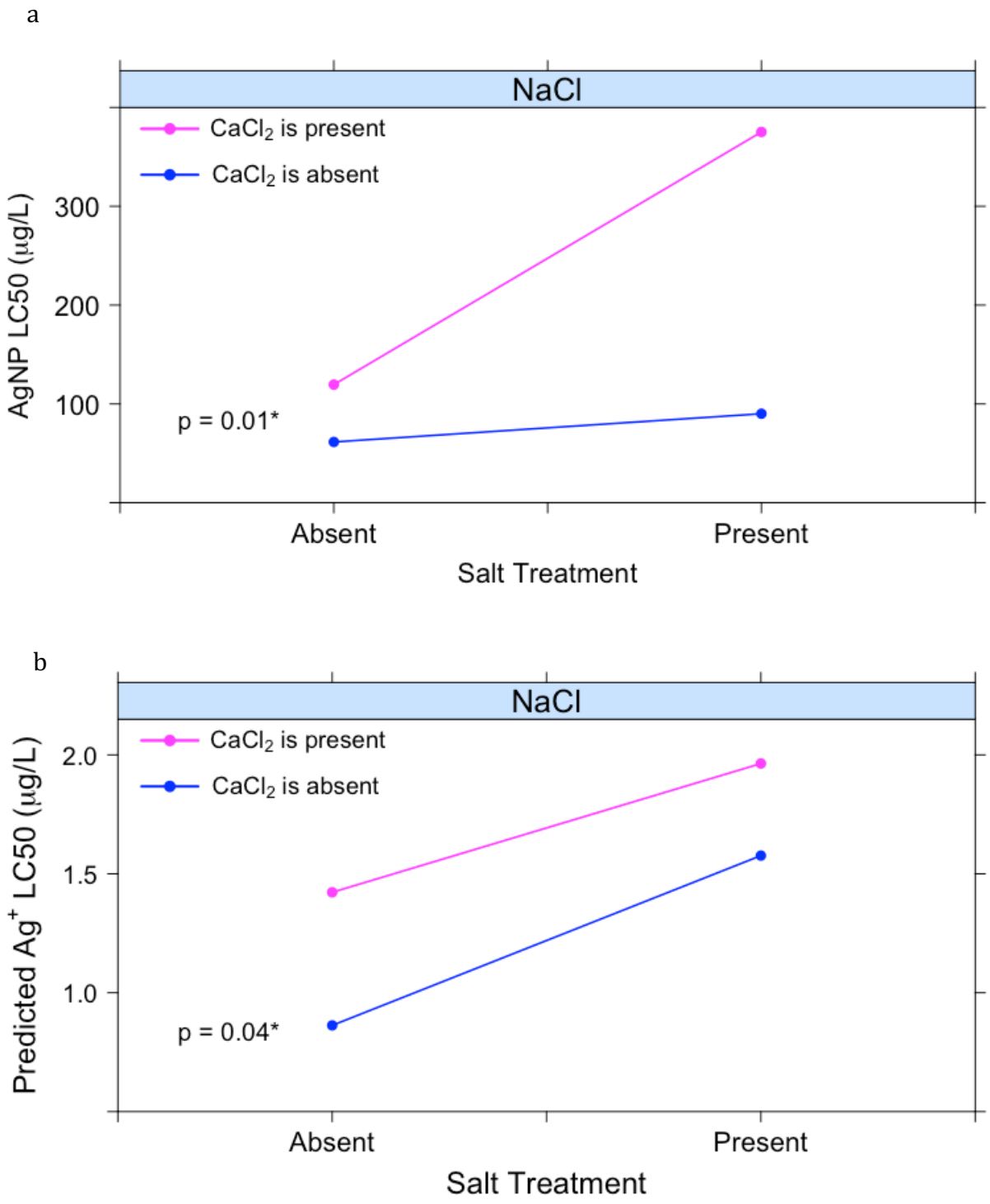

Figure 4. Analysis of interaction effects between NaCl and $CaCl_2$ in the factorial analyses of: a) measured AgNP LC50, and b) the BLM-predicted Ag^+ LC50. The interaction plots show the effect of the absence versus the presence of the NaCl treatment when the $CaCl_2$ treatment was absent (bottom line) versus present (top line). Asterisks indicate the interaction was significant.

Biotic Ligand Model

A brief summary of the BLM output can be found in Table 10 and the results of the factorial analysis on BLM-predicted Ag^+ LC50 in Table 11. Factorial analysis found all three salt treatments and the interaction between NaCl and $CaCl_2$ to significantly increase the BLM-predicted Ag^+ LC50 (Figures 4b, 5; Table A2). Free Ag^+ in solution decreased with increasing Cl^- concentrations from the salt treatments, while AgCl in solution increased with the Cl^--containing salt treatments (Table 10).

Table 10. Summarized BLM results for each experimental freshwater in order of ascending predicted Ag^+ LC50.

Water	Predicted Ag^+ LC50 (µg/L)	Predicted AgCl in solution (µg/L)	Predicted free Ag^+ in solution (µg/L)
MHW	0.810	0.101	0.733
NS	0.916	0.113	0.830
CC	1.34	1.07	0.468
NC	1.50	1.20	0.521
CC-NS	1.50	1.20	0.530
NC-NS	1.66	1.32	0.583
NC-CC	1.87	1.70	0.385
NC-CC-NS	2.06	1.87	0.431

Table 11. Descriptive statistics for selected BLM endpoints across all experimental waters. Significance from factorial analysis indicates whether a salt or interaction was significant (Y) or not (N).

	Descriptive Statistics				Significant in Factorial Analysis?					
	Mean	Median	Min	Max	NaCl	$CaCl_2$	Na_2SO_4	NaCl:$CaCl_2$	NaCl:Na_2SO_4	$CaCl_2$:Na_2SO_4
Ag^+ LC50 (µg/L)	1.46	1.50	0.809	2.06	Y	Y	Y	Y	N	N

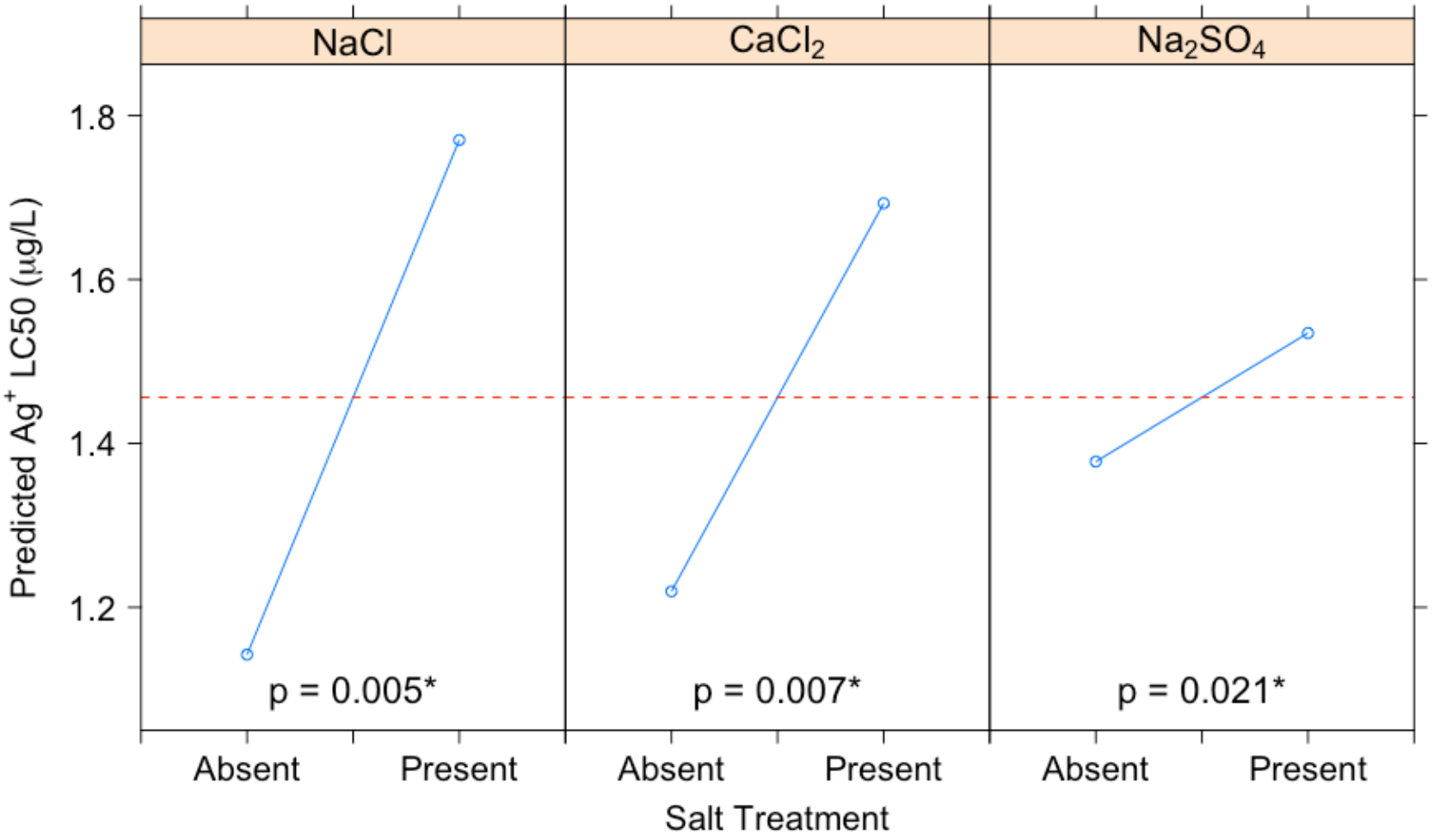

Figure 5. Main effects plots showing the effects that the BLM predicts the addition of the NaCl, $CaCl_2$, and Na_2SO_4 salt treatments would have on Ag^+ LC50 (present) compared to the waters without each respective salt treatments (absent). The respective factorial model is in Table A2. Asterisks indicate the salt factor was significant.

UV-Vis Spectrophotometry

The electrolyte composition of each experimental water significantly affected AgNP sedimentation patterns (Table 12; Figures 6, 7). Factorial analysis found that $CaCl_2$ was a significant factor ($p \leq 0.009$) affecting all three decay rate constants (k_{fast}, k_{medium}, and k_{slow}) in the fitted three-phase decay models (Table 13; Figure 8a-c). The medium rate constant was also significantly affected by NaCl ($p = 0.023$). Although NaCl and the interaction between NaCl and $CaCl_2$ were both nonsignificant for the fast rate, the inclusion of these terms in the factorial model ($p = 0.133$ and $p = 0.069$, respectively) improved the adjusted r-squared value from 0.747 to 0.889, so it is likely that the concentration of NaCl was slightly below a concentration that may have induced a strong enough effect to cross the α threshold (Table A3). Na_2SO_4 was nonsignificant for all rate constants. Factorial analysis on the plateaus predicted by each fitted model found all salt factors and interactions to be nonsignificant (Table 13; Figure 8d). Simple main effects contrasts found significant differences between waters at all compared times (Table 12) except 2 and 3.5 hrs (Figure 7). Significant differences between experimental waters were initially divided between the waters with $CaCl_2$ (CC, CC-NS, NC-CC, and NC-CC-NS; hereafter referred to as the Ca group) and the waters without $CaCl_2$ (MHW, NC, NS, and NC-NS; hereafter referred to as the no-Ca group).

Table 12. Average absorbance of AgNPs from UV-Vis spectrophotometry in each experimental water ± 1 standard deviation after different times throughout the 3.5 hr run time of the experiment (n = 5).

		Average absorbance					
		8 min	15 min	30 min	1 hr	2 hr	3.5 hr
		± ≤ 0.08807	± ≤ 0.06391	± ≤ 0.04048	± ≤ 0.02507	± ≤ 0.02411	± ≤ 0.02173
No-Ca Group	MHW	0.34205	0.29929	0.24640	0.19363	0.14976	0.12064
	NS	0.36925	0.31775	0.25627	0.19553	0.14743	0.11671
	NC	0.30032	0.25878	0.21167	0.16931	0.13156	0.10432
	NC-NS	0.28775	0.23365	0.17929	0.13478	0.10130	0.07925
Ca-Group	CC-NS	0.24023	0.20461	0.17389	0.14860	0.12613	0.10646
	NC-CC	0.19209	0.16840	0.14911	0.13155	0.11310	0.09464
	NC-CC-NS	0.18890	0.16448	0.14469	0.12708	0.10961	0.09321
	CC	0.18246	0.15713	0.13673	0.11933	0.10258	0.08723

Table 13. Selected model components from the exponential decay models for all experimental waters. Significance from factorial analysis indicates whether a salt or interaction was significant (Y) or not (N) on any of the three rate constants (k) or the predicted plateau.

		k_{fast} (sec^{-1})	k_{med} (sec^{-1})	k_{slow} (sec^{-1})	Plateau
No-Ca Group	MHW	0.7112	0.1294	0.02268	0.09485
	NS	0.6236	0.1262	0.02304	0.09001
	NC	2.763	0.2011	0.02775	0.08747
	NC-NS	0.5695	0.1594	0.02462	0.06146
Ca-Group	CC-NS	0.9712	0.1994	0.01917	0.08475
	NC-CC	1.573	0.2585	0.01617	0.06883
	NC-CC-NS	1.733	0.2750	0.02051	0.07742
	CC	1.370	0.2466	0.01970	0.07099
Significant in Factorial Analysis?	NaCl	N*	Y	N	N
	$CaCl_2$	Y	Y	Y	N
	Na_2SO_4	N	N	N	N
	NaCl:$CaCl_2$	N*	N	N	N
	NaCl:Na_2SO_4	N	N	N	N
	$CaCl_2$:Na_2SO_4	N	N	N	N

* Model term was nonsignificant ($0.05 < p < 0.15$) but inclusion in the factorial model improved adjusted r-squared value from 0.747 to 0.889.

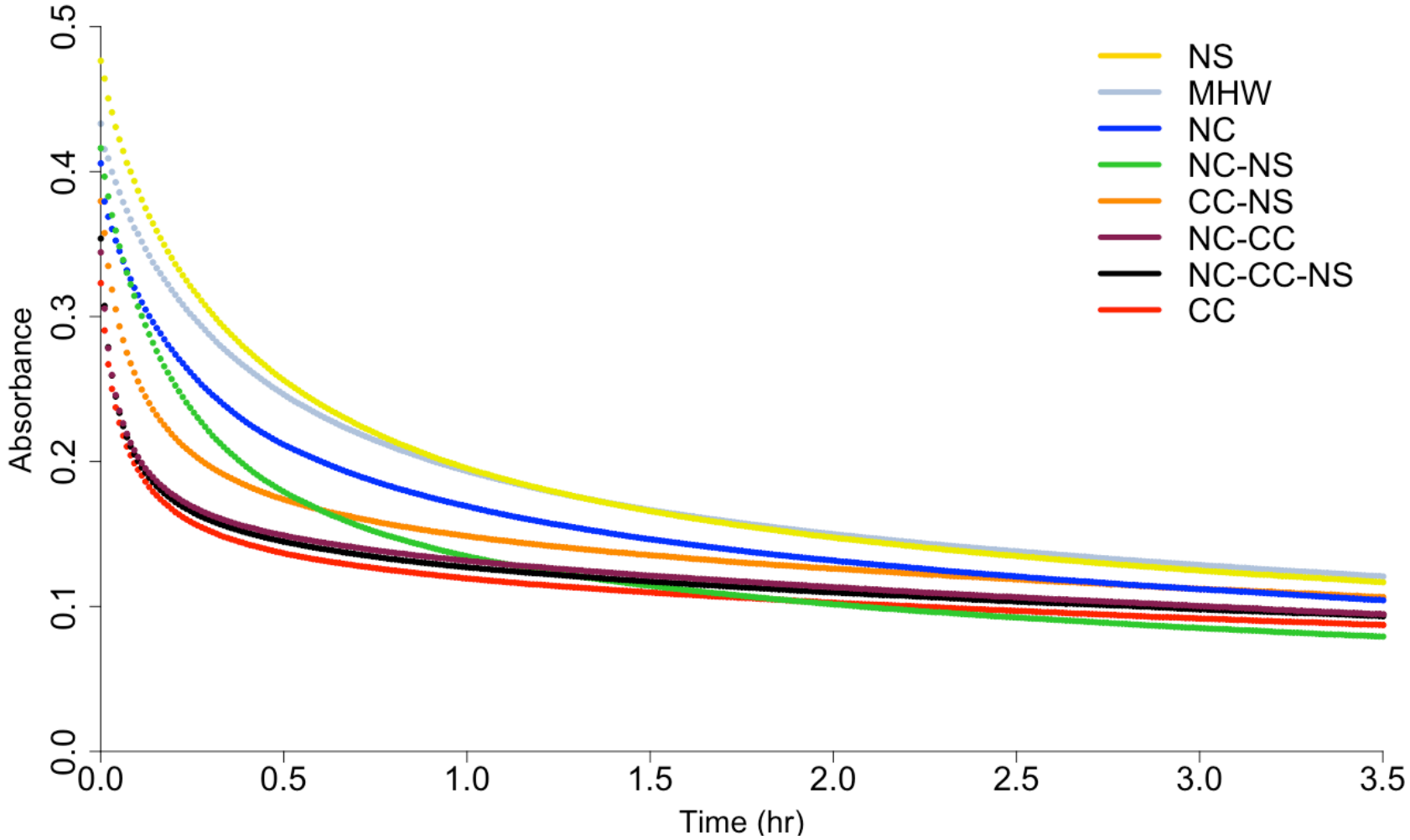

Figure 6. Average absorbance at λ = 416 nm of sedimenting AgNPs over time as measured using UV-Vis spectrophotometry (n = 5).

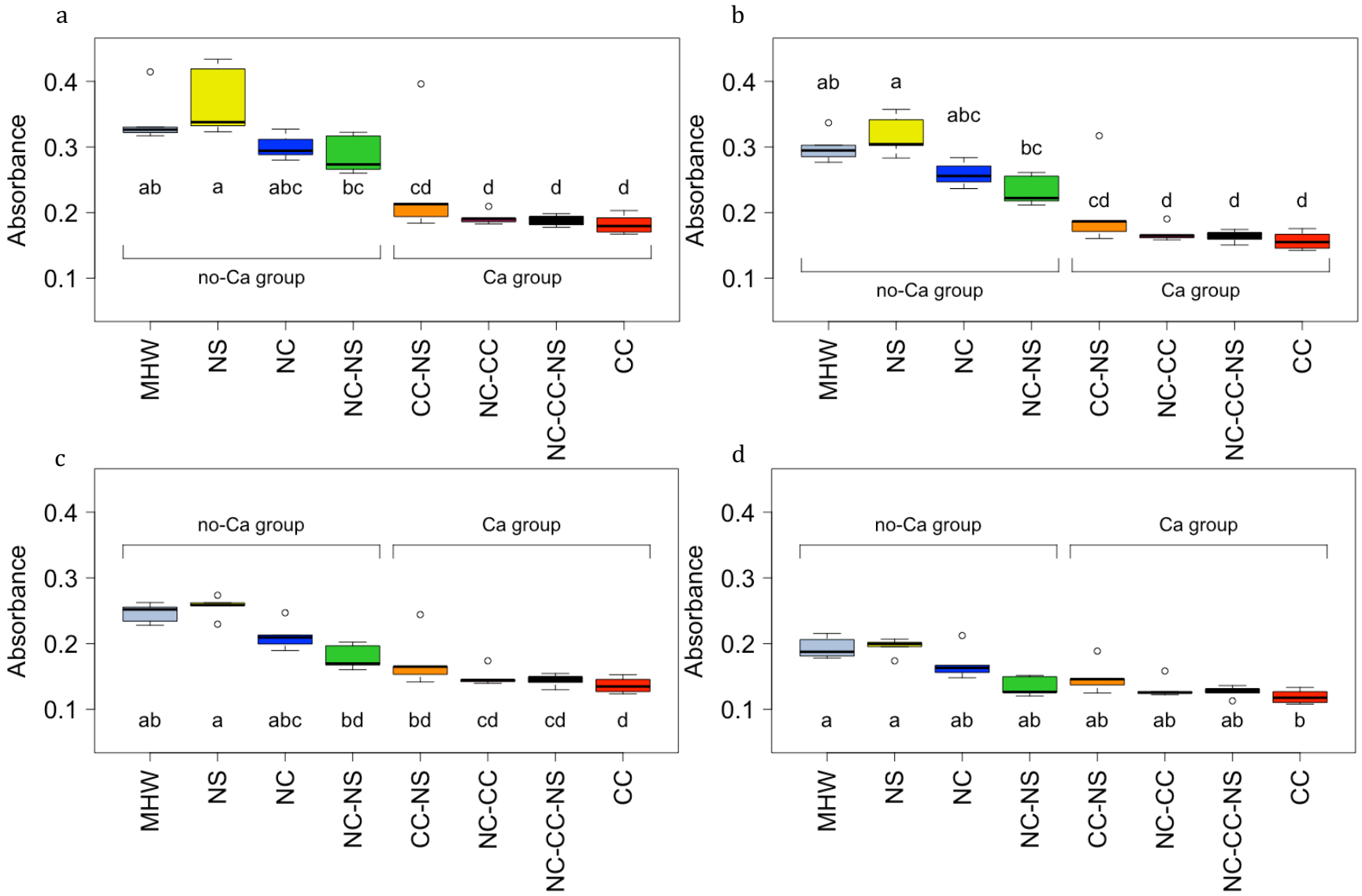

Figure 7. Light absorbed by AgNPs in each experimental water at λ = 416 nm measured using UV-Vis spectrophotometry after a) 8 min, b) 15 min, c) 30 min, and d) 1 hr. Letters indicate statistical groupings at each time calculated from simple main effects contrasts (family α = 0.05) (n = 5).

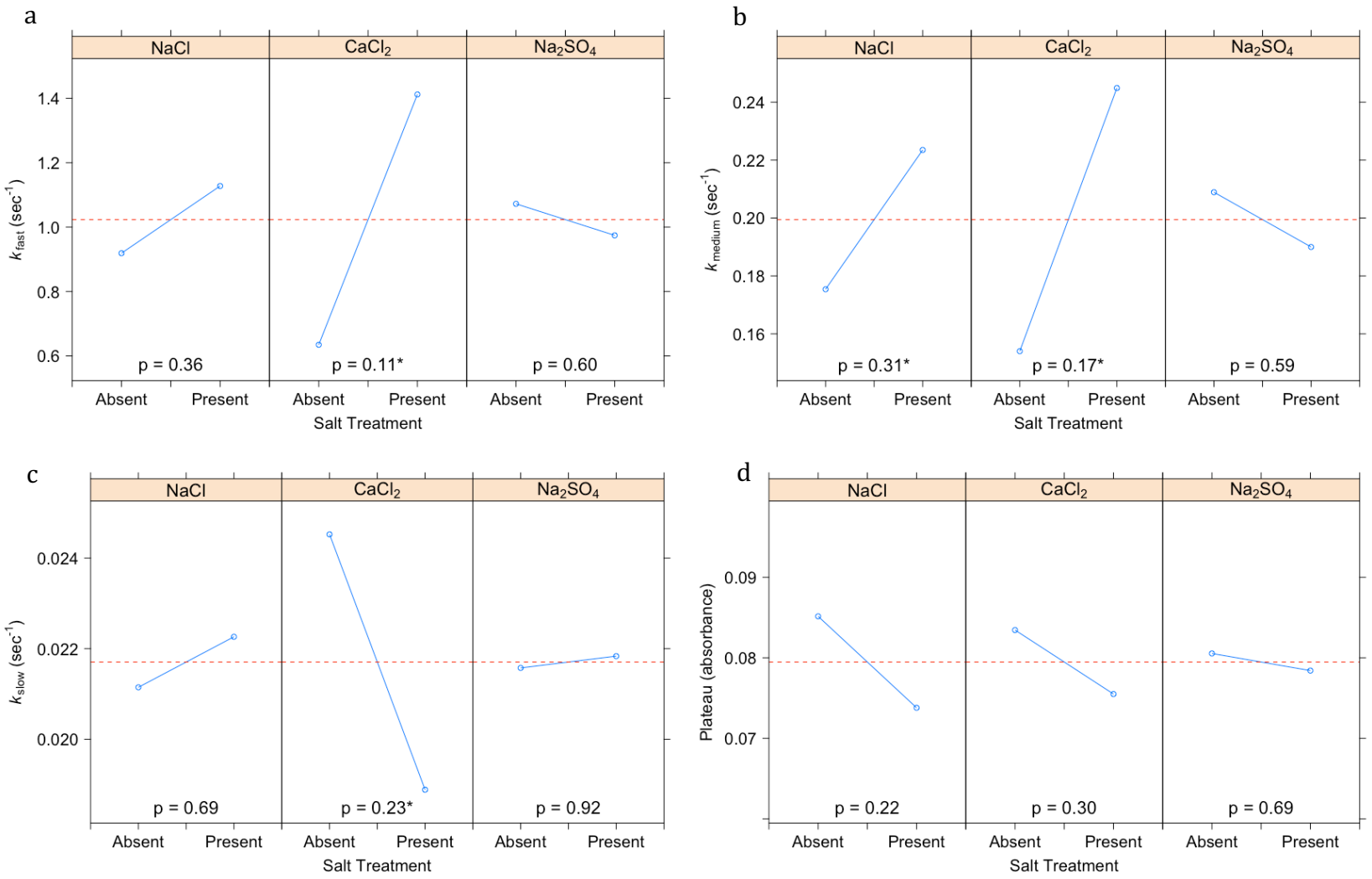

Figure 8. Main effects plots showing the effects that the NaCl, $CaCl_2$, and Na_2SO_4 salt treatments had on the sedimentation patterns measured on UV-Vis (present) compared to the waters without each respective salt treatment (absent). Factorial analyses were performed on selected model components of the three-phase decay models that were fit to the absorbance patterns of AgNPs in each experimental water: a) k_{fast}, b) k_{medium}, c) k_{slow}, and d) plateau. Final factorial models are in Tables A3 – A6. Asterisks indicate the salt factor was significant in the final model.

ICP-MS

Since ICP-MS measurements were made using LC50 concentrations for each experimental water, the two tests without toxicity results (NS and NC-CC-NS) were not measured on ICP-MS. Effect of AgNP batch on ICP-MS measurements was not able to be determined therefore statistical tests on ICP-MS particle size measurements were only conducted between measurements derived from the same synthesized AgNP batch (Table 8). NC-CC at 24 hrs was not included in analyses because it was isolated in a batch by itself.

Particle size distributions on ICP-MS revealed multimodal distributions in all experimental waters and at both measurement times (Figure 1). All distributions had some kind of particle presence that peaked between 30 – 45 nm, and at least one other distribution between 70 – 100 nm. In most samples, however, these main distributions were composed of multiple smaller distributions that indicate aggregation patterns within the larger distributions (Montano et al. 2016; Kim et al. 2017).

The comparisons based on AgNP batch resulted in seven separate X^2 tests for independence (Table 14). All tests found the existence of significant differences between AgNP distributions across the three size categories (< 60 nm, 60 – 100 nm, > 100 nm) with the exception of the distributions for MHW and MHW with NaCl (NC) after 3.5 hrs where no significant differences were found. Individual X^2 contingency tables can be found in Appendix B and are summarized in Table 14.

The same AgNP batch limitations on statistical comparisons were applied to particle concentration as a precaution. A two-way ANOVA comparing the effect of experimental water and time spent in the water between the CC, CC-NS, and NC-NS freshwaters, which

were all from the same batch, found experimental water ($F_{2,6}$ = 9.41, p = 0.014, generalized η^2 = 0.96) and time ($F_{1,6}$ = 7.47, p = 0.034, generalized η^2 = 0.89) to both significantly affect particle concentration. The interaction effect between water and time was nonsignificant ($F_{2,6}$ = 0.67, p = 0.55, generalized η^2 = 0.56), therefore time decreased particle concentration in all three waters the same way. The particle concentrations between MHW and the NC water were different after 3.5 hrs ($F_{1,2}$ = 117.89, p = 0.008, generalized η^2 = 0.94) but no difference was found between them after 24 hrs ($F_{1,2}$ = 17.56, p = 0.053, generalized η^2 = 0.75).

Since there was no indication whether AgNP batch did or did not affect particle concentration and no information from the literature on whether batch might have had an effect, a two-way ANOVA comparing all waters and times against each other (ignoring batch altogether) was also run. Information on particle concentration in relation to AgNP toxicity is extremely limited and of increasing interest and concern and the results of this test can provide insight to the discussion on nanoparticle toxicity and informed direction for future research using otherwise missing information. Thus, the two-way ANOVA comparing all tested waters across both measurement times found particle concentration to be significantly affected by experimental water ($F_{5,14}$ = 22.37, $p \ll 0.001$, η^2 = 0.94) and measurement time ($F_{1,14}$ = 38.43, $p \ll 0.001$, η^2 = 0.84). The interaction between water and time was nonsignificant ($F_{5,14}$ = 2.13, p = 0.132, η^2 = 0.59), reaffirming that time decreased particle concentration in experimental waters the same way. Pairwise t-tests comparing experimental waters found two distinct statistical groups (Figure 9a): MHW, CC-NS, NC, and CC were statistically similar despite AgNP nominal concentrations ranging from

52.29 – 118.52 µg/L; and NC-NS and NC-CC were statistically similar despite AgNP concentrations from 214.97 – 331.17 µg/L (Table 6).

The Pearson correlation tests were comparisons between particle concentrations and nominal LC50 values and were therefore not restricted by experimental batch limitations. Particle concentration and LC50 were positively correlated at both 3.5 hrs (Pearson's $r = 0.84$, $p = 0.001$), 24 hrs (Pearson's $r = 0.76$, $p = 0.004$), and for the combined readings of both times (Pearson's $r = 0.71$, $p < 0.001$) (Figure 9b).

Table 14. X^2 tests for independence performed between sample types (n = 2) by AgNP batch. If the X^2 statistic was significant (family $\alpha = 0.05$), a X^2 contingency analysis was performed to determine where differences between waters and size categories existed. X^2 contingency tables can be viewed in Appendix B.

AgNP Batch	Samples Compared	X^2 statistic	Significant?	Summary of Contingency Analysis
Batch 1	**3.5 hr:** MHW vs NC	5.07	No	Analysis not performed for nonsignificant X^2 statistic
Batch 2	**24 hr:** MHW vs NC	19.72	Yes	NC has more particles > 100 nm than MHW
Batch 3	**CC:** 3.5 hr vs 24 hr	37.89	Yes	24 hr samples had more particles > 100 nm than 3.5 hr samples, which had more particles between 60 - 100 nm
Batch 3	**CC-NS:** 3.5 hr vs 24 hr	60.95	Yes	24 hr samples had more particles > 100 nm than 3.5 hr samples, which had more particles between 60 - 100 nm
Batch 3	**NC-NS:** 3.5 hr vs 24 hr	15.42	Yes	24 hr samples had more particles > 100 nm than 3.5 hr samples
Batch 3	**3.5 hr:** CC vs CC-NS vs NC-NS vs NC-CC	76.68	Yes	NC-CC (n = 1) had many more particles > 100 nm than the hypothetical expected distribution and substantially fewer between 60 - 100 nm. NC-NS (n = 1) showed the opposite (few particles > 100 nm and many between 60 - 100 nm)
Batch 3	**24 hr:** CC vs CC-NS vs NC-NS	134.30	Yes	The waters with $CaCl_2$ had significantly higher distributions of AgNPs > 100 nm than NC-NS, which had a much higher distribution of particles between 60 - 100 nm

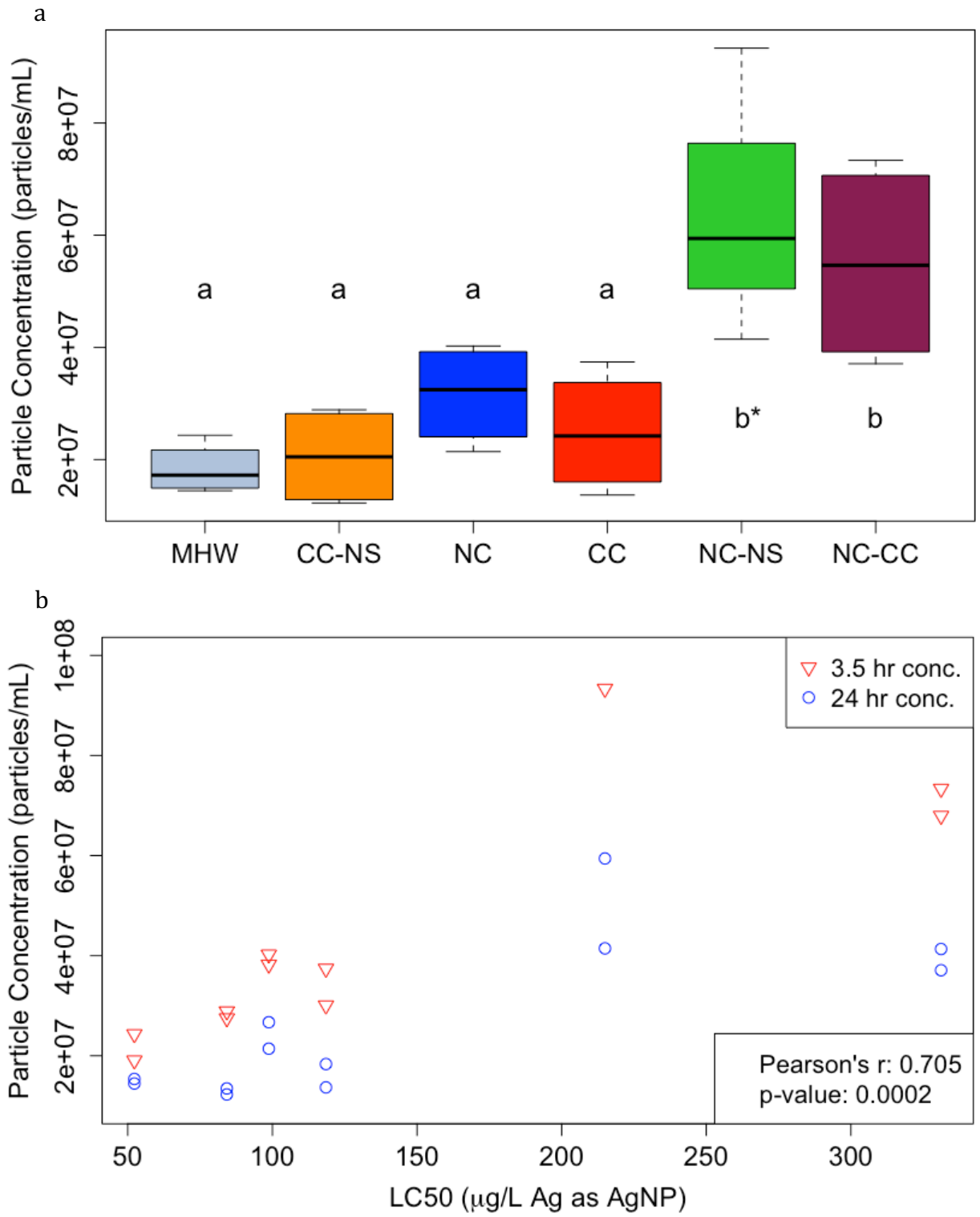

Figure 9. a) Particle concentrations from ICP-MS at LC50 concentrations in each water at 3.5 and 24 hrs. Waters are in ascending LC50 order. Letters signify statistical groupings, however, the possible effects of AgNP batch were ignored in this two-way ANOVA. The * on the letter for NC-NS is because of a missing replicate for 3.5 hrs. b) Particle concentration after 3.5 and 24 hrs of exposure in experimental waters against the nominal LC50 (Table 6) of that water.

Discussion

Toxicity

The LC50 concentrations observed in this study, which ranged from 53.48 – 383.52 µg/L (Figure 2), are consistent with other ranges that have been reported for citrate-capped AgNPs greater than or equal to 40 nm: Seitz et al. (2015) found 60 nm citrate AgNPs in pH 8.0 to result in EC50s between 75 – 120 µg/L; Cui et al. (2015) measured a mean *D. magna* EC50 at 44.83 µg/L for 55 nm PVP-capped AgNPs; and Conine et al. (2017) measured LC50s for 30 – 50 nm AgNPs between 34 – 292 µg/L on wild daphnia neonates from various boreal lakes whose water was the test media.

The NaCl and $CaCl_2$ salt treatments both significantly reduced AgNP toxicity in this study (Figure 3) (the Na_2SO_4 treatment was not able to be evaluated), and also elicited an interaction effect (Table A1). The dissociated ions from these salts (Na^+, Ca^{2+}, and Cl^-) induce AgNP aggregation according to other studies (e.g. Huynh and Chen 2011; Baalousha et al. 2013; Chen and Zhang 2014), which has been shown to reduce the Ag^+ concentration in solution (Zhang et al. 2011; Li and Lenhart 2012; Yue et al. 2015). Reduced Ag^+ from the particle surface decreases the toxicity of the AgNPs (Kennedy et al. 2010; Li and Lenhart 2012; Harmon et al. 2014; Groh et al. 2015; Li et al. 2015).

The dissociated ions from the salt treatments also reduce the aquatic toxicity of Ag^+ to *D. magna* at the biotic ligand (Di Toro et al. 2001; Bielmeyer et al. 2007; Naddy et al. 2017). Factorial analysis of the BLM-predicted Ag^+ LC50 in each experimental water found that the BLM predicted all three salt treatments to significantly reduce Ag^+ toxicity (Figure 5) and also found an interaction effect between NaCl and $CaCl_2$ (Table A2). The rank order of AgNP LC50s observed in this study was the same as the rank order of LC50s

that the BLM predicted should occur for Ag^+ toxicity in each experimental water (when nonsignificant differences in measured CC-NS, NC, and CC LC50s were considered) (Table 15). The matching rank order indicates that Ag^+ dissolved from the AgNP surface may have been responsible for some component of the AgNP toxicity in this study. However, differences between how the BLM predicted the salt treatments would affect Ag^+ toxicity and what was actually observed for AgNP toxicity suggests that the BLM does not sufficiently characterize all of the factors that affect AgNP toxicity. Specifically, the $CaCl_2$ treatment had a larger effect on the AgNP LC50 than the NaCl treatment (Figure 3), which was opposite what the BLM predicted would occur for just Ag^+ toxicity (Figure 5). Additionally, the NaCl and $CaCl_2$ interaction effect observed for AgNP LC50 reduced toxicity substantially more than the effect that the BLM predicted would occur for just Ag^+ toxicity (Figure 4). Of particular note is the ratio comparing the observed AgNP LC50 to the BLM-predicted Ag^+ LC50 for each water (Table 15), which shows AgNP LC50s were not consistent with the BLM. MHW, CC-NS, and NC each resulted in a AgNP LC50 that was 56 – 66 times the BLM-predicted Ag^+ LC50, but CC, NC-NS, and NC-CC resulted in AgNP LC50s with ratios that increased progressively higher than that. Consistent ratios suggest that AgNP LC50 was correlated with Ag^+ toxicity predicted by the BLM, therefore the increase in ratio for the waters with higher AgNP LC50s indicates that there were AgNP-specific behaviors acting on toxicity in this study.

Table 15. AgNP LC50 concentrations in ascending rank order alongside LC50 statistical group, average particle concentration, corresponding BLM-predicted Ag^+ LC50s, and the ratio of the AgNP LC50 and the BLM-predicted Ag^+ LC50.

	AgNP LC50 (µg/L)	AgNP LC50 statistical group	Average Particle Concentration (particles/mL)	BLM-predicted Ag^+ LC50 (µg/L)	Ratio of AgNP LC50 : BLM LC50
MHW	53.48	a	1.84×10^7	0.81	66.02
CC-NS	84.20	b	2.09×10^7	1.50	56.13
NC	97.75	b	3.35×10^7	1.50	65.17
CC	118.69	b	2.56×10^7	1.34	88.57
NC-NS	217.16	c	6.61×10^7	1.66	130.82
NC-CC	383.52	d	5.82×10^7	1.87	205.09

UV-Vis

The sedimentation of AgNPs was significantly affected by the addition of the $CaCl_2$ and NaCl salt treatments (Figure 6). DLVO theory clearly explains why $CaCl_2$ was significant in particle size and sedimentation analyses; increased collision success, via the masking of the EDL from the presence of Ca^{2+}, created larger aggregates over shorter periods of time (Li et al. 2010; Baalousha et al. 2013; He et al. 2013; Chen and Zhang et al. 2014). This is most clearly observable in Figures 6 and 7, which exhibit particle sedimentation in each experimental water. AgNPs in the Ca-group waters (CC, CC-NS, NC-CC, and NC-CC-NS) were all in a statistical group characterized by significantly lower absorbances than the waters in the no-Ca group (MHW, NC, NS, and NC-NS) after both 8 and 15 minutes because such a large proportion of aggregates in the Ca-group waters had already sedimented out of the water column. In contrast, the AgNPs in the no-Ca group waters were aggregating and sedimenting more slowly due to reduced collision success from the absence of Ca^{2+} masking the EDL. The absorbance readings for waters in the no-Ca group took between 30

min and two hrs to be statistically similar to waters in the Ca-group because more AgNPs were still present in the water column.

In the no-Ca group, the two waters that had NaCl (NC and NC-NS) caused AgNPs to sediment more rapidly than the other two no-Ca waters that did not have NaCl (MHW and NS) (Figures 6, 7). DLVO theory describes how Na^+ can also screen the EDL, albeit less effectively than Ca^{2+} (Huynh and Chen 2011; Baalousha et al. 2013; Chen and Zhang 2014). The presence of Cl^- with the NaCl addition also provides an explanation for increased sedimentation rates due to its ability to bridge AgNPs together into aggregates from AgCl precipitation on the AgNP surfaces (Li et al. 2010; Ameer et al. 2014; Chambers et al. 2014). The aggregating effects from the NaCl salt treatment could have been caused by either ion or a combination of the effects of both.

Na_2SO_4 did not significantly affect any of the analyzed decay model components. This salt treatment added the same concentration of Na^+ as the NaCl treatment (Table 2) therefore the absence of significant effects from Na_2SO_4 indicates that either: the added Na^+ concentration was too low to have EDL screening abilities and the ion affecting particle behavior for NaCl was entirely the Cl^-, or the SO_4^{2-} had a particle-stabilizing property that counteracted the EDL screen from the concentration of Na^+ added with the Na_2SO_4 treatment. Because the effects of the SO_4^{2-} could not be determined, the differences in effects observed from NaCl versus Na_2SO_4 in this study were not able to be isolated to the specific ions in either salt.

The interaction effect that occurred between NaCl and $CaCl_2$ on the fast sedimentation rate (Table 12) was likely due to a compounding effect of increased Cl^- concentration. Baalousha et al. (2013) and He et al. (2013) both found Ca^{2+} to be

50 – 63 times more efficient at AgNP aggregation than Na^+, and Baalousha et al. (2013) concluded further that, even in a NaCl:$CaCl_2$ ratio of 50:1, the aggregating effects of Na^+ were negligible in the presence of Ca^{2+}. The ratio of Na^+:Ca^{2+} in this study was 2:1 (Table 3). The addition of Na^+ in the presence of relatively high Ca^{2+} should have had no effect on particle behaviors, therefore the interaction effects observed between NaCl and $CaCl_2$ can reasonably be attributed to the properties of the Cl^-.

ICP-MS

The aggregating abilities of Ca^{2+} were also observable in the particle size distributions from the ICP-MS. The CC and CC-NS waters revealed significantly higher distributions of larger particle aggregates than the NC-NS water after both 3.5 and 24 hrs (Tables B6-B7). Although Cl^- has been shown to also have particle aggregating abilities (El Badawy et al. 2010; Li et al. 2010; Baalousha et al. 2013), the NC-NS water had the same Cl^- concentration as the other two waters, but it was added as NaCl rather than $CaCl_2$ (Tables 2-3). The difference in particle size distributions between these three waters can therefore be specifically isolated to the effect of the Ca^{2+} from the $CaCl_2$.

The NaCl salt treatment also significantly increased AgNP aggregate size but, as with the UV-Vis sedimentation results, was less effective than the $CaCl_2$ treatment. In comparison to MHW, the NC water showed substantial aggregation across its particle size distribution after 24 hrs (Tables 13, B2), but not after just 3.5 hrs (Tables 13, B1). The introduction of NaCl induced aggregation, but it took time before it was observable. When both the NaCl and $CaCl_2$ treatments were added (forming the NC-CC water), the distribution of large aggregates was much higher than the waters with only one of those

salt treatments (Table B6). The 2:1 ratio of Na^+ to Ca^{2+} concentrations in this study (Table 2) means the Na^+ should have had no effect on AgNP aggregation in the presence of the Ca^{2+} (Baalousha et al. 2013; He et al. 2013). The increased aggregation observed in the NC-CC water can therefore be attributed to the doubled Cl^- concentration.

This study did not find conclusive evidence on whether or not particle concentration had any relationship with AgNP toxicity, however most observed patterns between particle concentration and toxicity suggest that it did not. The particle concentration range of the MHW LC50 (53.48 µg/L) was statistically similar to the particle concentration ranges of the CC-NS, NC, and CC waters (Figure 9a), which had LC50s 1.6 – 2.2 times higher than the MHW LC50 (Table 15). This similarity in particle concentration at 50% mortality despite significant differences in the LC50 concentrations expressed as mass Ag indicates that particle aggregation and sedimentation in the waters with added salt treatments may have been reducing the overall particle concentration in the water column and lends support to the idea that a component of toxicity could be related to particle concentration; the same particle concentrations appear to have elicited the same levels of toxicity. However, NC-NS and NC-CC had LC50 particle concentration ranges that were significantly higher than the other four waters (which would not have happened if toxicity corresponded with particle concentration). Additionally, the significant positive correlation between particle concentration and LC50 (Figure 9b) shows that when higher concentrations of AgNPs were added at the start of the ICP-MS tests, higher particle concentrations were measured. This pattern indicates that the statistical groupings of the LC50 particle concentrations for each water were a direct result of the experimental set-up of the ICP-MS tests and how close

LC50 concentrations were to one another rather than an indication that similar particle concentrations were eliciting the same toxic response.

Conclusions

The aggregation and sedimentation of AgNPs in this study may have reduced AgNP toxicity. The $CaCl_2$ salt treatment significantly affected particle behaviors, and these behaviors, which were not observed for the NaCl treatment, may be responsible for why the $CaCl_2$ treatment had a stronger effect on reducing AgNP toxicity than the NaCl treatment. The interaction effect on particle behaviors observed between NaCl and $CaCl_2$ may also be responsible for the exaggerated size of the NaCl and $CaCl_2$ interaction effect observed for AgNP toxicity, which was much higher than what the BLM predicted would occur for just Ag^+ toxicity. Reduced toxicity from particle aggregation and sedimentation may also be responsible for the progressively increasing LC50 ratios. Particle aggregation and sedimentation rates are affected by collision frequency, which increases at higher particle concentrations (Piccapietra et al. 2012; Baalousha et al. 2013; He et al. 2013; Kim et al. 2017; McGillicuddy et al. 2017). Waters that required higher concentrations of AgNPs to overwhelm the protection of the relevant salt treatments at the biotic ligand would have consequently been affected by increased rates of aggregation and sedimentation, which could have reduced the AgNP toxicity even further through reduced Ag^+ dissolution. These findings ultimately support that the BLM is not able to adequately account for all of the factors that influence toxicity when nanoparticles are present.

This study shows that the ions in current aquatic toxicity media may have large or small effects on AgNP behavior and toxicity and that those effects may change depending

on the other ions present in the test media. The composition of testing media should be selected intentionally with consideration as to how individual ions may affect the results of AgNP tests. Regardless of recipe, this study proves the critical importance of publishing detailed water chemistry information alongside AgNP toxicity results, including the ion composition of the testing media. Reports without this information risk their results being misinterpreted by audiences that are unaware of the sensitive nature of AgNPs and can be of limited use to audiences that wish to compare results against those of other studies.

The significant effects of the NaCl and $CaCl_2$ salt treatments on the aggregation and sedimentation behaviors of the AgNPs suggest that AgNPs transported to environments with elevated concentrations of the dissociated ions will exhibit similar behaviors. This study showed that these ions reduced the toxicity of the AgNPs to freshwater organisms that inhabit the water column, however removal of the AgNPs from the water column via the sedimentation process may instead increase AgNP exposure to benthic organisms. This benthic exposure may be exacerbated in marine environments where ion concentrations are much higher than in freshwater ecosystems.

References

Ameer, F. S.; Zhou, Y.; Zou, S.; Zhang, D. Wavelength-dependent correlations between ultraviolet-visible intensities and surface enhanced raman spectroscopic enhancement factors of aggregated gold and silver nanoparticles. *Journal of Physical Chemistry C*. **2014**. *118*, 22234-22242.

Asghari, S.; Johari, S. A.; Lee, J. H.; Kim, Y. S.; Jeon, Y. B.; Choi, H. J.; Moon, M. C.; Yu, I. J. Toxicity of various silver nanoparticles compared to silver ions in *Daphnia magna*. *Journal of Nanobiotechnology*. **2012**. *10*, 14.

ASTM. *Standard Guide for Conducting Acute Toxicity Tests on Test Materials with Fishes, Macroinvertebrates, and Amphibians*; Method E 729-96; ASTM International: Conshohocken, Pa, **2014**, www.astm.org.

ASTM. *Standard Guide for Conducting Daphnia magna Life-Cycle Toxicity Tests*; Method E 1193-97; ASTM International: Conshohocken, PA, **2012**, www.astm.org.

Baalousha, M.; Nur, Y.; Römer, I.; Tejamaya, M.; Lead, J. R. Effect of monovalent and divalent cations, anions and fulvic acid on aggregation of citrate-coated silver nanoparticles. *Science of the Total Environment*. **2013**. *454*, 119-131.

Beer, C.; Foldbjerg, R.; Hayashi, Y.; Sutherland, D. S.; Autrup, H. Toxicity of silver nanoparticles—Nanoparticle or silver ion? *Toxicology Letters*. **2012**. *208*, 286-292.

Behra, R.; Sigg, L.; Clift, M. J. D.; Herzog, F.; Minghetti, M.; Johnston, B.; Petri-Fink, A.; Rothen-Rutishauser, B. Bioavailability of silver nanoparticles and ions: from a chemical and biochemical perspective. *Journal of the Royal Society Interface*. **2013**. *10* (87), 20130396.

Bielmeyer, G. K.; Grosell, M.; Paquin, P. R.; Mathews, R.; Wu, K. B.; Santore, R. C.; Brix, K. V. Validation study of the acute biotic ligand model for silver. *Environmental Toxicology and Chemistry*. **2007**. *26* (10): 2241-2246.

Berthouex, P. M.; Brown, L. C. Factorial Experimental Designs. *Statistics for Environmental Engineers*; CRS Press, Inc/Lewis Publishers: Boca Raton, FL, 1994; pp 151-160.

Bi, X.; Lee, S.; Ranville, J. F.; Sattigeri, P.; Spanias, A.; Herckes, P.; Westerhoff, P. Quantitative resolution of nanoparticle sizes using single particle inductively coupled plasma mass spectrometry with the K-means clustering algorithm. *Journal of Analytical Atomic Spectrometry*. **2014**. *29*, 1630-1639.

Biotic Ligand Model, version 3.36.2.45; Windward Environmental LLC, 2018, http://www.windwardenv.com/biotic-ligand-model/.

Bhui, D. K.; Bar, H.; Sarkar, P.; Sahoo, G. P.; De, S. P.; Misra, A. Synthesis and UV-vis spectroscopic study of silver nanoparticles in aqueous SDS solution. *Journal of Molecular Liquids*. **2009**. *145*, 33-37.

Chambers, B. A.; Afrooz, A. R. M. N.; Bae, S.; Aich, N.; Katz, L.; Seleh, N. B.; Kirisits, M. J. Effects of chloride and ionic strength on physical morphology, dissolution, and bacterial toxicity of silver nanoparticles. *Environmental Science & Technology*. **2014**. *48*, 761-769.

Chen, K. L.; Elimelech, M. Aggregation and deposition kinetics of fullerene (C60) nanoparticles. *Langmuir*. **2006**. *22*, 10994-11001.

Chen, S.-F.; Zhang, H. Stability and sedimentation of silver nanoparticles in the presence of monovalent, divalent, and trivalent electrolyte solutions. *Water Science & Technology*. **2014**. *70* (2), 361-366.

Chikramane, P. S.; Suresh, A. K.; Kane, S. G.; Bellare, J. R. Metal nanoparticle induced hermetic activation: a novel mechanism of homeopathic medicines. *Homeopathy*. **2017**. *106*, 135-144.

Conine, A. L.; Frost, P. C. Variable toxicity of silver nanoparticles to *Daphnia magna*: effects of algal particles and animal nutrition. *Ecotoxicology*. **2017**. *26*, 118-126.

Conine, A. L.; Rearick, D. C.; Xenopoulos, M. A.; Frost, P. C. Variable silver nanoparticle toxicity to *Daphnia* in boreal lakes. *Aquatic Toxicology*. **2017**. *192*, 1-6.

Croteau, M-N.; Dybowska, Ag. D.; Luoma, S. N.; Misra, S. K.; Valsami-Jones, E. Isotopically modified silver nanoparticles to assess nanosilver bioavailability and toxicity at environmentally relevant exposures. *Environmental Chemistry*. **2014**. *11*, 247-256.

Cui, R.; Chae, Y.; An, Y-J. Dimension-dependent toxicity of silver nanomaterials on the cladocerans *Daphnia magna* and *Daphnia geleata*. *Chemosphere*. **2017**. *185*, 205-212.

Cupi, D.; Hartmann, N. B.; Baun, A. Influence of pH and media composition on a suspension stability of silver, zinc oxide, and titanium dioxide nanoparticles and immobilization of *Daphnia magna* under guideline testing conditions. *Ecotoxicology and Environmental Safety*. **2016**. *127*, 144-152.

Degueldre, C.; Favarger, P.-Y. Colloid analysis by single particle inductively coupled plasma-mass spectroscopy: A feasibility study. *Colloids and Surfaces A: Physicochemical and Engineering Aspects*. **2003**. *217*, 137-142.

Degueldre, C.; Favarger, P.-Y. Thorium colloid analysis by single particle inductively coupled plasma-mass spectrometry. *Talenta*. **2004**. *62*, 1051-1054.

Degueldre, C.; Favarger, P.-Y.; Bitea, C. Zirconia colloid analysis by single particle inductively coupled plasma-mass spectrometry. *Analytica Chimica Acta*. **2004**. *518*, 137-142.

Degueldre, C.; Favarger, P.-Y.; Rossé, R.; Wold, S. Uranium colloid analysis by single particle inductively coupled plasma-mass spectrometry. *Talenta*. **2006a**. *68*, 623-628.

Degueldre, C.; Faverger, P.-Y.; Wold, S. Gold colloid analysis by inductively coupled plasma-mass spectrometry in a single particle mode. *Analytica Chimica Acta*. **2006b**. *555*, 263-268.

Di Toro, D. M.; Allen, H. E.; Bergman, H. L.; Meyer, J. S.; Paquin, P. R.; Santore, R. C. Biotic ligand model of the acute toxicity of metals. 1. Technical basis. *Environmental Toxicology & Chemistry*. **2001**. *20* (10), 2383-2396.

El Badawy, A.; Luxton, T. P.; Silva, R. G.; Scheckel, K. G.; Suidan, M. T.; Tolaymat, T. M. Impact of environmental conditions (pH, ionic strength, and electrolyte type) on the surface charge and aggregation of silver nanoparticles suspensions. *Environmental Science & Technology*. **2010**. *44*, 1260-1266.

Ellis, L.-J. A.; Baalousha, M.; Valsami-Jones, E.; Lead, J. R. Seasonal variability of natural water chemistry affects the fate and behavior of silver nanoparticles. *Chemosphere*. **2018**. *191*, 616-625.

Fabrega, J.; Luoma, S. N.; Tyler, C. R.; Galloway, T. S.; Lead, J. R.' Silver nanoparticles: Behaviour and effects in the aquatic environment. *Environmental International*. **2011**, *37*, 517-531.

Furtado, L. M.; Hoque, M. E.; Mitrano, D. F.; Ranville, J. F.; Cheever, B.; Frost, P. C.; Xenopoulos, M. A.; Hintelmann, H.; Metcalfe, C. D. The persistence and transformation of silver nanoparticles in littoral lake mesocosms monitored using various analytical techniques. *Environmental Chemistry*. **2014**. *11* (4), 419-430.

Gao, J.; Youn, S.; Hovsepyan, A.; Llaneza, V. L.; Wang, Y.; Bitton, G.; Bonzongo, J.-C. J. Dispersion and toxicity of selected manufactured nanomaterials in natural water samples: Effects of water chemical composition. *Environmental Science & Technology*. **2009**. *43*, 3322-3328.

Garcia-Alonso, J.; Khan, F. R.; Misra, S. K.; Turmaine, M.; Smith, B. D.; Rainbow, P. S.; Luoma, S. N.; Valsami-Jones, E. Cellular internalization of silver nanoparticles in gut epithelia of the estuarine polychaete *Nereis diversicolor*. *Environmental Science & Technology*. **2011**. *45*, 4630-4636.

Gebauer, J. S.; Treuel, L. Influence of individual ionic components on the agglomeration kinetics of silver nanoparticles. *Journal of Colloid and Interface Science*. **2011**. *354*, 546-554.

Gonçalves, S. F.; Pavlaki, M. D.; Lopes, R.; Hammes, J.; Gallego-Urrea, J. A.; Hassellöv, M.; Jurkschat, K.; Crossley, A.; Loureiro, S. Effects of silver nanoparticles on the freshwater snal *Physa acuta*: The role of test media and snails' life cycle stage. *Environmental Toxicology and Chemistry*. **2017**. *36* (1), 243-253.

Gottschalk, F.; Sun, T.; Nowack, B. Environmental concentrations of engineered nanomaterials: Review of modeling and analytical studies. *Environmental Pollution*. **2013**. *181*, 287-300.

Graphpad QuickCalcs Outlier Calculator. http://www.graphpad.com/quickcalcs/grubbs1/ (accessed Aug, 2018).

Groh, K. J.; Dalkvist, T.; Piccapietra, F.; Behra, R.; Suter, M. J.-F.; Schirmer, K. Critical influence of chloride ions on silver ion-mediated acute toxicity of silver nanoparticles to zebrafish embryos. *Nanotoxicology*. **2015**. *9* (1), 81-91.

Harmon, A. R.; Kennedy, A. J.; Poda, A. R.; Bednar, A. J.; Chappell, M. A.; Steevens, J. A. Determination of nanosilver dissolution kinetics and toxicity in an environmentally relevant aqueous medium. *Environmental Toxicology and Chemistry*. **2014**, *33* (8), 1783-1791.

He, D.; Bligh, M. W.; Waite, T. D. Effects of aggregate structure on the dissolution kinetics of citrate-stabilized silver nanoparticles. *Environmental Science & Technology*. **2013**. *47*, 9148-9156.

Hicks, A. L.; Gibertson, L. M.; Yamani, J. S.; Theis, T. L.; Zimmerman, J. B. Life cycle payback estimates of nanosilver enabled textiles under different silver loading, release, and laundering scenarios informed by literature review. *Environmental Science & Technology*. **2015**. *49*, 7529-7542.

Hu, T.; Chen, X.; Yang, K.; Lin, D. Distinct toxicity of silver nanoparticles and silver nitrate to *Daphnia magna* in M4 medium and surface water. *Science of the Total Environment*. **2018**. *618*, 838-846.

Hull, M.; Kennedy, A. J.; Detzel, C.; Vikesland, P.; Chappell, M. A. Moving beyond mass: The unmet need to consider dose metrics in environmental nanotoxicology studies. *Environmental Science & Technology*. **2012**. *46*, 10881-10882.

Huynh, K. A.; Chen, K. L. Aggregation kinetics of citrate and polyvinylpyrrolidone coated silver nanoparticles in monovalent and divalent electrolyte solutions. *Environmental Science & Technology*. **2011**. *45*, 5564-5571.

ISO. *Water quality—Determination of the inhibition of the mobility of* Daphnia magna *Straus (*Cladocera, Crustacea*)—Acute toxicity test*; Method 6341:2012(E); International Organization for Standardization: Geneva, Switzerland, **2012**, www.iso.org.

Ivask, A.; Kurvet, I.; Kasemets, K.; Blinova, I.; Aruoja, V.; Suppie, S.; Vija, H.; Käkinen, A.; Titma, T.; Heinlaan, M.; Visnapuu, M.; Koller, D.; Kisand, V.; Kahru, A. Size-dependent toxicity of silver nanoparticles to bacteria, yeast, algae, crustaceans and mammalian cells *in vitro*. *PLOS One*. **2014**. *9* (7), e102108.

Jiménez-Lamana, J.; Slaveykova, V. I. Silver nanoparticle behavior in lake water depends on their surface coating. *Science of the Total Environment*. **2016**. *573*, 946-953.

Kennedy, A. J.; Hull, M. S.; Bednar, A. J.; Goss, J. D.; Gunter, J. C.; Bouldin, J. L.; Vikesland, P. J.; Steevens, J. A. Fractionating nanosilver: Importance for determining toxicity to aquatic test organisms. *Environmental Science & Technology*. **2010**. *44*, 9571-9577.

Kennedy, A. J.; Hull, M. S.; Diamond, S.; Chappell, M.; Bednar, A. J.; Laird, J. G.; Melby, N. L.; Steevens, J. A. Gaining a critical mass: A dose metric conversion case study using silver nanoparticles. *Environmental Science & Technology*. **2015**. *49*, 12490-12499.

Khan, F. R.; Paul, K. B.; Dybowska, A. D.; Valsami-Jones, E.; Lead, J. R.; Stone, V.; Fernandes, T. F. Accumulation dynamics and acute toxicity of silver nanoparticles to *Daphnia magna* and *Lumbriculus variegatus*: Implications for metal modeling approaches. *Environmental Science & Technology*. **2015**. *49*, 4389-4397.

Kidd, J. M.; Hanigan, D.; Truong, L.; Hristovski, K.; Tanguay, R.; Westerhoff, P. Developing and interpreting aqueous functional assays for comparative property-activity relationships of different nanoparticles. *Science of the Total Environment*. **2018**. *628*, 1609-1616.

Kim, H.-A.; Lee, B.-T.; Na, S.-Y.; Kim, K.-W.; Ranville, J. F.; Kim, S.-O.; Jo, E.; Eom, I.-C. Characterization of silver nanoparticle aggregates using single particle-inductively coupled plasma-mass spectrometry (spICP-MS). *Chemosphere*. **2017**. *171*, 468-475.

Kittler, S.; Greulich, C.; Diendorf, J.; Köller, M.; Epple, M. Toxicity of silver nanoparticles increases during storage because of slow dissolution under release of silver ions. *Chemistry of Materials*. **2010**. *22*, 4548-4554.

Lee, P. C.; Meisel, D. Adsorption and surface-enhanced raman of dyes on silver and gold sols. *The Journal of Physical Chemistry*. **1982**. *86* (17), 3391-3395.

Lee, K. J.; Nallathamby, P. D.; Browning, L. M.; Osgood, C. J.; Xu, X.-H. N. *In vivo* imaging of transport and biocompatibility of single silver nanoparticles in early development of zebrafish embryos. *ACS Nano*. **2007**. *1* (2), 133-143.

Lee, Y.-J.; Kim, J.; Oh, J.; Bae, S.; Lee, S.; Hong, I. S.; Kim, S.-H. Ion-release kinetics and ecotoxicity effects of silver nanoparticles. *Environmental Toxicology and Chemistry*. **2012**. *31* (1), 155-159.

Li, X.; Lenhart, J. J.; Walker, H. W. Dissolution-accompanied aggregation kinetics of silver nanoparticles. *Langmuir*. **2010**. *26* (22), 16690-16698.

Li, X.; Lenhart, J. L. Aggregation and dissolution of silver nanoparticles in natural surface water. *Environmental Science & Technology*. **2012**. *46*, 5378-5386.

Li, M.; Lin, D.; Zhu, L. Effects of water chemistry on the dissolution of ZnO nanoparticles and their toxicity of *Escherichia coli*. *Environmental Pollution*. **2013**. 173: 97-102.

Li, L.; Wu, H.; Ji, C.; van Gestel, C. A. M.; Allen, H. E.; Peijnenburg, W. J. G. M. A metabolomic study on the responses of *Daphnia magna* exposed to silver nitrate and coated silver nanoparticles. *Ecotoxicology and Environmental Safety*. **2015**. *119*, 66-73.

Limpiteepraken, P.; Babel, S. Leaching potential of silver from nanosilver-treated textile products. *Environmental Monitoring and Assessment*. **2016**. *188*, 156.

Liu, J.; Hurt, R. H. Ion release kinetics and particle persistence in aqueous nano-silver colloids. *Environmental Science & Technology*. **2010**. *44* (6), 2169-2175.

Liu, W.; Zhou, Q.; Liu, J.; Fu, J.; Liu, S.; Jiang, G. Environmental and biological influences on the stability of silver nanoparticles. *Chinese Science Bulletin*. **2011**. *56* (19), 2009-2015.

Lorenz, C.; Windler, L.; von Goetz, N.; Lehmann, R. P.; Schuppler, M.; Hungerbühler, K.; Heuberger, M.; Nowack, B. Characterization of silver release from commercially available functional (nano)textiles. *Chemosphere*. **2012**, *89*, 817-824.

Loza, K.; Diendorf, J.; Sengstock, C.; Ruiz-Gonzalez, L.; Gonzalez-Calbet, J. M.; Vallet-Regi, M.; Köller, M.; Epple, M. The dissolution and biological effects of silver nanoparticles in biological media. *Journal of Materials Chemistry B*. **2014**. *2*, 1634.

McGillicuddy, E.; Murray, I.; Kavanagh, S.; Morrison, L.; Fogarty, A.; Cormican, M.; Dockery, P.; Predergast, M.; Rowan, N.; Morris, D. Silver nanoparticles in the environment: Sources, detection and ecotoxicology. *Science of the Total Environment*. **2017**. *575*, 231-246.

McLaughlin, J.; Bonzongo, J.-C. J. Effects of natural water chemistry on nanosilver behavior and toxicity to *Ceriodaphnia dubia* and *Pseudokirchneriella subcapitata*. *Nanomaterials in the Environment*. **2012**. *31* (1), 168-175.

Meesters, J. A. J.; Veltman, K.; Hendriks, A. J.; van de Meent, D. Environmental exposure assessment of engineered nanoparticles: Why REACH needs adjustment. *Integrated Environmental Assessment and Management*. **2013**, *9* (3), e15-e26.

Merrifield, R. C.; Stephan, C.; Lead, J. Determining the concentration dependent transformations of Ag nanoparticles in complex media: Using SP-ICP-MS and Au@Ag core-shell nanoparticles as tracers. *Environmental Science & Technology*. **2017**. *51*, 3206-3213.

Minghetti, M.; Schirmer, K. Effect of media composition on bioavailability and toxicity of silver and silver nanoparticles in fish intestinal cells (RTgutGC). *Nanotoxicology*. **2016**. *10* (10), 1526-1534.

Mitrano, D. M.; Lesher, E. K.; Bednar, A.; Monserud, J.; Higgins, C. P.; Ranville, J. F. Detecting nanoparticulate silver using single-particle inductively coupled plasma-mass spectrometry. *Nanomaterials in the Environment*. **2012**. *31* (1), 115-121.

Miyashita, S.-i.; Mitsuhashi, H.; Fujii, S.-i.; Takatsu, A.; Inagaki, K.; Fujimoto, T. High transport efficiency of nanoparticles through a total-consumption sample introduction system and its beneficial application for particle size evaluation in single-particle ICP-MS. *Analytical and Bioanalytical Chemistry*. **2017**. *409*, 1531-1545.

Molleman, B.; Hiemstra, T. Surface structure of silver nanoparticles a model for understanding the oxidative dissolution of silver ions. *Langmuir*. **2015**. *31*, 13361-13372.

Montano, M. D.; Badiei, H. R.; Bazargan, S.; Ranville, J. F. Improvements in the detection and characterization of engineered nanoparticles using spICP-MS with microsecond dwell times. *Environmental Science: Nano*. **2014**. *1* (4), 338-346.

Montano, M. D.; Olesik, J. W.; Barber, A. G.; Challis, K.; Ranville, J. F. Single particle ICP-MS: Advances toward routine analysis of nanomaterials. *Analytical and Bioanalytical Chemistry*. **2016**. *408*, 5053-5074.

Naddy, R. B.; Stubblefield, W. A.; Bell, R. A.; Wu, K. B.; Santore, R. C.; Paquin, P. R. Influence of varying water quality parameters on the acute toxicity of silver to the freshwater cladoceran, *Ceriodaphnia dubia*. *Bulletin of Environmental Contamination and Toxicology*. **2018**. *100*: 69-75.

Navarro, E.; Piccapietra, F.; Wagner, B.; Marconi, F.; Kaegi, R.; Odzak, N.; Sigg, L.; Behra, R. Toxicity of silver nanoparticles to *Chlamydomonas reinhardtii*. *Environmental Science & Technology*. **2008a**. *42*, 8959-8964.

Navarro, E.; Baun, A.; Nehra, R.; Hartmann, N. B.; Filser, J.; Miao, A.-J.; Quigg, A.; Santschi, P.H.; Sigg, L. Environmental behavior and ecotoxicity of engineered nanoparticles to algae, plants, and fungi. *Ecotoxicology*. **2008b**. *17*, 372-386.

NIST/SEMATECH. 5.4.7.1. Full factorial example. In *e-Handbook of Statistical Methods*, 2013, http://www.itl.nist.gov/div898/handbook/ (accessed July 2018).

NIST/SEMATECH. 5.5.9.8. Half-normal probability plot. In *e-Handbook of Statistical Methods*, 2013, http://www.itl.nist.gov/div898/handbook/ (accessed July 2018).

NIST Reference Material 8013, Gold Nanoparticles nominal 60 nm diameter Report of Investigation. http://www-s.nist.gov/srmors/view_cert.cfm?srm-8013 (accessed July 2018).

OECD. *Test No. 202: Daphnia sp., Acute Immobilization Test*; Organisation for Economic Co-operation and Development: Paris, **2004**. www.oecd.org.

Pace, H. E.; Rogers, N. J.; Jarolimek, C.; Coleman, V. A.; Higgins, C. P.; Ranville, J. F. Determining transport efficiency for the purpose of counting and sizing nanoparticles via single particle inductively coupled plasma mass spectrometry. *Analytical Chemistry*. **2011**. *83*, 9361-9369.

Pace, H. E.; Rogers, N. J.; Jarolimek, C.; Coleman, V. A.; Higgins, C. P.; Ranville, J. F. Correction to determining transport efficiency for the purpose of counting and sizing nanoparticles via single particle inductively coupled plasma mass spectrometry. *Analytical Chemistry*. **2012**. *84*, 4633-4633.

Park, J.-W.; Oh, J.-H.; Kim, W.-K.; Lee, S.-K. Toxicity of citrate-coated silver nanoparticles differs according to method of suspension preparation. *Bulletin of Environmental Contamination and Toxicology*. **2014**. *93*, 53-59.

Peterson, E. J.; Diamond, S. A.; Kennedy, A. J.; Goss, G. G.; Ho, K.; Lead, J.; Hanna, S. K.; Hartmann, N. B.; Hund-Rinke, K.; Mader, B.; Manier, N.; Pandard, P.; Salina, E. R.; Sayre, P. Adapting OECD aquatic toxicity tests for use with manufactured nanomaterials: Key issues and consensus recommendations. *Environmental Science & Technology*. **2015**. *49*, 9532-9547.

Piccapietra, F.; Sigg, L.; Behra, R. Colloidal stability of carbonate-coated silver nanoparticles in synthetic and natural freshwater. *Environmental Science & Technology*. **2012**. *46*, 818-825.

Pillai, Z. S.; Kamat, P. V. What factors control the size and shape of silver nanoparticles in the citrate ion reduction method? *Journal of Physical Chemistry B*. **2004**. *108*, 945-951.

Pokhrel, L. R.; Dubey, B.; Scheuerman P. R. Impacts of select organic ligands on the colloidal stability, dissolution dynamics, and toxicity of silver nanoparticles. *Environmental Science & Technology*. **2013**. *47*, 12877-12885.

Poynton, H. C.; Lazorchak, J. M.; Impellitteri, C. A.; Blalock, B. J.; Rogers, K.; Allen, H. J.; Loguinov, A.; Heckman, J. L.; Govindasmawy, S. Toxicogenomic responses of nanotoxicity in *Daphnia magna* exposed to silver nitrate and coated silver nanoparticles. *Environmental Science & Technology*. **2012**. *46*, 6288-6296.

Prism, version 7; Graphpad, 2017.

R Core Team. R: A language and environment for statistical computing. R Foundation for Statistical Computing, Vienna, Austria, 2018, http://www.R-project.org/.

Ritz, C.; Strebig, J. C. drc: Analysis of Dose-Response Curves, version 3.0-1; 2016.

Roe, A. L. Collosol argentum and its ophthalmic uses. *The British Medical Journal*. **1915**. 104.

Römer, I.; Gavin, A. J.; White, T. A.; Merrifield, R. C.; Chipman, J. K.; Viant, M. R.; Lead, J. R. The critical importance of defined media conditions in *Daphnia magna* nanotoxicity studies. *Toxicology Letters*. **2013**. *233*, 103-108.

Sakamoto, M.; Ha, J.-Y.; Yoneshima, S.; Kataoka, C.; Tatsuta, H.; Kashiwada, S. Free silver ion as the main cause of acute and chronic toxicity of silver nanoparticles to cladocerans. *Archives of Environmental Contamination and Toxicology*. **2015**. *68* (3), 500-509.

Sakka, Y.; Skjolding, L. M.; Mackevica, A.; Filser, J.; Baun, A. Behavior and chronic toxicity of two differently stabilized silver nanoparticles to *Daphnia magna*. *Aquatic Toxicology*. **2016**. *177*, 526-535.

Schäfer, B.; vom Brocke, J.; Epp, A.; Götz, M.; Herzberg, F.; Kneuer, C.; Sommer, Y.; Tentschert, J.; Noll, M.; Günther, I.; Banasiak, U.; Böl, G. F.; Lampen, A.; Luch, A.; Hensel, A. State of the art in human risk assessment of silver compounds in consumer products: a conference report on silver and nanosilver held at the BfR in 2012. *Archives of Toxicology*. **2013**. *87*, 2249-2262.

Sharma, V. K.; Yngard, R. A.; Yekaterina, L. Silver nanoparticles: Green synthesis and their antimicrobial activities. *Advances in Colloid and Interface Science*. **2009**. *145*, 83-96.

Shen, M.-H.; Zhou, X.-X.; Yang, X.-Y.; Chao, J.-B.; Liu, R.; Liu, J.-F. Exposure medium: Key in identifying free Ag+ as the exclusive species of silver nanoparticles with acute toxicity to *Daphnia magna*. *Scientific Reports*. **2015**. *5*, 9674.

Schultz, A. G.; Ong, K. J.; MacCormack, T.; Ma, G.; Veinot, J. G. C.; Goss, G. G. Silver nanoparticles inhibit sodium uptake in juvenile rainbow trout (*Oncorhynchus mykiss*). *Environmental Science & Technology*. **2012**. *46* (18), 10295-10301.

Schultz, A. G.; Boyle, D.; Chamot, D.; Ong, K. J.; Wilkinson, K. J.; McGeer, J. C.; Sunahara, G.; Goss, G. G. Aquatic toxicity of manufactured nanomaterials: challenges and recommendations for future toxicity testing. *Environmental Chemistry*. **2014**. *11*, 207-226.

Stebounova, L. V.; Guio, E.; Grassian, V. H. Silver nanoparticles in simulated biological media: a study of aggregation, sedimentation, and dissolution. *Journal of Nanoparticle Research*. **2011**. *13*, 233-244.

Stevenson, L. M.; Krattenmaker, K. E.; Johnson, E.; Bowers, A. J.; Adeleye, A. S.; McCauley, E.; Nisbet, R. M. Standardized toxicity testing may underestimate ecotoxicity: Environmentally relevant food rations increase the toxicity of silver nanoparticles to *Daphnia*. *Environmental Toxicology and Chemistry*. **2017**. *36* (11), 3008-3018.

Tejamaya, M.; Römer, I.; Merrifield, R. C.; Lead, J. R. Stability of citrate, PVP, and PEG coated silver nanoparticles in ecotoxicology media. *Environmental Science & Technology*. **2012**. *46*, 7011-7017.

Tolaymat, T. M.; El Badawy, A. M.; Genaidy, A.; Scheckel, K. G.; Luxton, T. P.; Suidan, M. An evidence-based environmental perspective of manufactured silver nanoparticle in synthesis and applications: A systematic review and critical appraisal of peer-reviewed scientific papers. *Science of the Total Environment*. **2010**. *408*, 999-1006.

Unrine, J. M.; Colman, B. P.; Bone, A. J.; Gondikas, A. P.; Matson, C. W. Biotic and abiotic interactions in aquatic microcosms determine fate and toxicity of Ag nanoparticles. Part 1. Aggregation and dissolution. *Environmental Science & Technology*. **2012**. *46*, 6915-6924.

US EPA. *Methods for measuring the acute toxicity of effluents and receiving waters to freshwater and marine organism*; Fifth Edition; Method EPA-821-R-02-012; U.S. Environmental Protection Agency: Washington, DC, **2002**.

Xiu, Z.; Zhang, Q.; Puppala, H. L.; Colvin, V. L.; Alvarez, P. J. J. Negligible particle-specific antibacterial activity of silver nanoparticles. *Nano Letters*. **2012**. *12*, 4271-4275.

Yue, T.; Behra, R.; Sigg, L.; Freire, P. F.; Pillai, S.; Schirmer, K. Toxicity of silver nanoparticles to a fish gill cell line: Role of medium composition. *Nanotoxicology*. **2015**. *9* (1), 54-63.

Zhang, W.; Yao, Y.; Sullivan, N.; Chen, Y. Modeling the primary size effects of citrate-coated silver nanoparticles on their ion release kinetics. *Environmental Science & Technology*. **2011**. *45*, 4422-4428.

Zook, J. M.; Long, S. E.; Cleveland, D.; Geronimo, C. L. A.; MacCuspie, R. I. Measuring silver nanoparticle dissolution in complex biological and environmental matrices using UV-visible absorbance. *Analytical and Bioanalytical Chemistry*. **2011**. *401* (6), 1993-2002.

Appendix A: Factorial Analysis Tables

Final models with significant factors and interactions from factorial analyses on measured endpoints.

Table A1: Two-factor factorial analysis on measured LC50s for AgNP toxicity comparing NaCl and $CaCl_2$. n = 2. All factors and the interaction were significant.

	Df	Sum Sq	Mean Sq	F value	Pr(>F)	
NaCl	1	40421	40421	31.22	0.00503	**
CaCl2	1	58897	58897	45.49	0.00252	**
NaCl:CaCl2	1	25796	25796	19.92	0.01113	*
Residuals	4	5179	1295			

Multiple R-squared: 0.9602, Adjusted R-squared: 0.9304
F-statistic: 32.21 on 3 and 4 DF, p-value: 0.002923

Table A2: Three-factor factorial analysis on predicted LC50 for Ag^+ toxicity by the BLM.

	Df	Sum Sq	Mean Sq	F value	Pr(>F)	
NaCl	1	0.7971	0.7971	1132.70	5.77e-05	***
CaCl2	1	0.4541	0.4541	645.27	0.000134	***
Na2SO4	1	0.0492	0.0492	69.91	0.003587	**
NaCl:CaCl2	1	0.0153	0.0153	21.74	0.018616	*
Residuals	3	0.0021	0.0007			

Multiple R-squared: 0.9984, Adjusted R-squared: 0.9963
F-statistic: 467.4 on 4 and 3 DF, p-value: 0.0001602

Table A3: Three-factor factorial analysis on the fast rate (k_{fast}) of the modeled three-phase decay rate for AgNP sedimentation measured on using UV-Vis.

	Df	Sum Sq	Mean Sq	F value	Pr(>F)	
NaCl	1	0.0870	0.0870	3.541	0.13303	
CaCl2	1	1.2076	1.2076	49.144	0.00218	**
NaCl:CaCl2	1	0.1500	0.1500	6.103	0.06891	.
Residuals	4	0.0983	0.0246			

```
---
Multiple R-squared:  0.9363,  Adjusted R-squared:  0.8885
F-statistic:  19.6 on 3 and 4 DF,  p-value: 0.007446
```

Table A4: Three-factor factorial analysis on the medium rate (k_{medium}) of the modeled three-phase decay rate for AgNP sedimentation measured using UV-Vis.

```
            Df   Sum Sq  Mean Sq F value  Pr(>F)
NaCl         1 0.004627 0.004627   10.70 0.02218 *
CaCl2        1 0.016507 0.016507   38.17 0.00162 **
Residuals    5 0.002162 0.000432
---
Multiple R-squared:  0.9072,  Adjusted R-squared:  0.8701
F-statistic: 24.43 on 2 and 5 DF,  p-value: 0.002625
```

Table A5: Three-factor factorial analysis on the slow rate (k_{slow}) of the modeled three-phase decay rate for AgNP sedimentation measured using UV-Vis.

```
            Df    Sum Sq   Mean Sq F value  Pr(>F)
CaCl2        1 6.351e-05 6.351e-05   14.23 0.00926 **
Residuals    6 2.678e-05 4.460e-06
---
Multiple R-squared:  0.7034,  Adjusted R-squared:  0.654
F-statistic: 14.23 on 1 and 6 DF,  p-value: 0.009263
```

Table A6: Three-factor factorial analysis on the predicted plateau of the modeled three-phase decay rate for AgNP sedimentation measured using UV-Vis.

```
             Df    Sum Sq   Mean Sq F value Pr(>F)
NaCl          1 0.0002579 0.0002579   8.059  0.216
CaCl2         1 0.0001264 0.0001264   3.950  0.297
Na2SO4        1 0.0000090 0.0000090   0.282  0.689
NaCl:CaCl2    1 0.0000874 0.0000874   2.731  0.346
NaCl:Na2SO4   1 0.0000867 0.0000867   2.710  0.348
CaCl2:Na2SO4  1 0.0003538 0.0003538  11.056  0.186
Residuals     1 0.0000320 0.0000320
```

```
Multiple R-squared:  0.9664,  Adjusted R-squared:  0.765
F-statistic: 4.798 on 6 and 1 DF,  p-value: 0.3359
```

Appendix B: X^2 contingency tables for particle size distributions by size category measured on ICP-MS.

For tables B2-7, "Observed" indicates the averaged number of particle events in each size category (n = 2 unless otherwise indicated). "Expected" indicates the number of particles that would be in each size category if the size distributions were the same. "Residuals" describes the strength and direction of the deviation between observed and expected counts. "p-values" notes whether the difference between the waters in that size category was significant (α = 0.05). Significant p-values are bolded.

Table B1: X^2 statistic, and p-value comparing particle size distributions between MHW and the NC water after 3.5 hrs. X^2 value was nonsignificant, therefore no contingency table was run for this test.

X^2 statistic	p-value
5.07002	0.07926

Table B2: X^2 contingency table comparing the number of particles distributed across three size categories between the MHW and the NC water after 24 hrs. The waters are significantly different in the > 100 nm category.

Observed:	< 60 nm	60 - 100 nm	> 100 nm
MHW 24 hr	214	377	173.5
NC 24 hr	193	311.5	246
Expected:	< 60 nm	60 - 100 nm	> 100 nm
MHW 24 hr	205.4	347.4	211.7
NC 24 hr	201.6	341.1	207.8
Residuals	< 60 nm	60 - 100 nm	> 100 nm
MHW 24 hr	0.6	1.59	-2.62
NC 24 hr	-0.61	-1.6	2.65
p-values:	< 60 nm	60 - 100 nm	> 100 nm
MHW 24 hr	0.274	0.056	**0.004**
NC 24 hr	0.272	0.055	**0.004**

Table B3: X^2 contingency table comparing the number of particles distributed across three size categories of the CC water after 3.5 and 24 hrs. There was an increase in particles in the > 100 nm category after 24 hrs and a decrease of particles in the 60 – 100 nm category.

Observed:	< 60 nm	60 - 100 nm	> 100 nm
CC 3.5 hr	157	349.5	124
CC 24 hr	205.5	427.5	323.5
Expected:	< 60 nm	60 - 100 nm	> 100 nm
CC 3.5 hr	144	308.7	177.8
CC 24 hr	218.5	468.3	269.7
Residuals	< 60 nm	60 - 100 nm	> 100 nm
CC 3.5 hr	1.08	2.32	-4.03
CC 24 hr	-0.88	-1.89	3.28
p-values:	< 60 nm	60 - 100 nm	> 100 nm
CC 3.5 hr	0.140	**0.010**	**< 0.001**
CC 24 hr	0.190	**0.030**	**0.001**

Table B4: X^2 contingency table comparing the number of particles distributed across three size categories of the CC-NS water after 3.5 and 24 hrs. There was an increase in particles in the > 100 nm category after 24 hrs and a decrease of particles in the 60 – 100 nm category.

Observed:	< 60 nm	60 - 100 nm	> 100 nm
CC-NS 3.5 hr	148.5	330.5	95.5
CC-NS 24 hr	159.5	344.5	281
Expected:	< 60 nm	60 - 100 nm	> 100 nm
CC-NS 3.5 hr	130.2	285.2	159.1
CC-NS 24 hr	177.8	389.8	217.4
Residuals	< 60 nm	60 - 100 nm	> 100 nm
CC-NS 3.5 hr	1.61	2.68	-5.04
CC-NS 24 hr	-1.38	-2.29	4.31
p-values:	< 60 nm	60 - 100 nm	> 100 nm
CC-NS 3.5 hr	0.054	**0.004**	**≪ 0.001**
CC-NS 24 hr	0.084	**0.011**	**≪ 0.001**

Table B5: X^2 contingency table comparing the number of particles distributed across three size categories of the NC-NS water after 3.5 and 24 hrs. n = 1 for the 3.5 hr sample. The 24 hr samples were the only replicates where a KS-Test found a significant difference. There was no reason to doubt the legitimacy of either sample so size categories were still averaged. There was a significant increase in particles in the > 100 nm category after 24 hrs but no other significant differences between the distributions.

Observed:	< 60 nm	60 - 100 nm	> 100 nm
NC-NS 3.5 hr	180	436	67
NC-NS 24 hr	309.5	780	211
Expected:	< 60 nm	60 - 100 nm	> 100 nm
NC-NS 3.5 hr	168.6	418.7	95.7
NC-NS 24 hr	320.9	797.3	182.3
Residuals	< 60 nm	60 - 100 nm	> 100 nm
NC-NS 3.5 hr	0.88	0.84	-2.94
NC-NS 24 hr	-0.64	-0.61	2.13
p-values:	< 60 nm	60 - 100 nm	> 100 nm
NC-NS 3.5 hr	0.189	0.199	**0.002**
NC-NS 24 hr	0.261	0.27	**0.017**

Table B6: X^2 contingency table comparing the number of particles distributed across three size categories between the CC, CC-NS, NC-NS, and NC-CC waters after 3.5 hrs. For the NC-CC and NC-NS waters, n = 1. The NC-NS water had significantly fewer particles in the > 100 nm category and more in the 60 – 100 nm category than any of the other waters. The NC-CC water had significantly more particles in the > 100 nm category and fewer in the 60 – 100 nm category than any of the other waters.

Observed:	< 60 nm	60 - 100 nm	> 100 nm
CC 3.5 hr	157	349.5	124
CC-NS 3.5 hr	148.5	330.5	95.5
NC-NS 3.5 hr	180	436	67
NC-CC 3.5 hr	203	346	198
Expected:	< 60 nm	60 - 100 nm	> 100 nm
CC 3.5 hr	164.7	349.8	115.9
CC-NS 3.5 hr	150.1	318.8	105.6
NC-NS 3.5 hr	178.5	379	125.6
NC-CC 3.5 hr	195.2	414.5	137.4
Residuals	< 60 nm	60 - 100 nm	> 100 nm
CC 3.5 hr	-0.60	-0.02	0.75
CC-NS 3.5 hr	-0.13	0.66	-0.99
NC-NS 3.5 hr	0.12	2.93	-5.23
NC-CC 3.5 hr	0.56	-3.36	5.17
p-values:	< 60 nm	60 - 100 nm	> 100 nm
CC 3.5 hr	0.273	0.493	0.227
CC-NS 3.5 hr	0.448	0.255	0.162
NC-NS 3.5 hr	0.454	**0.002**	**< 0.001**
NC-CC 3.5 hr	0.288	**< 0.001**	**< 0.001**

Table B7: X^2 contingency table comparing the number of particles distributed across three size categories between the CC, CC-NS, and NC-NS, waters after 24 hrs. The NC-NS water had significantly fewer particles in the > 100 nm category and more in the 60 – 100 nm category than either of the other two waters.

Observed:	< 60 nm	60 - 100 nm	> 100 nm
CC 24 hr	205.5	427.5	323.5
CC-NS 24 hr	159.5	344.5	281
NC-NS 24 hr	309.5	780	211
Expected:	< 60 nm	60 - 100 nm	> 100 nm
CC 24 hr	212.1	488	256.4
CC-NS 24 hr	174.1	400.5	210.4
NC-NS 24 hr	288.4	663.5	348.6
Residuals	< 60 nm	60 - 100 nm	> 100 nm
CC 24 hr	-0.45	-2.74	4.19
CC-NS 24 hr	-1.10	-2.8	4.86
NC-NS 24 hr	1.24	4.52	-7.37
p-values:	< 60 nm	60 - 100 nm	> 100 nm
CC 24 hr	0.326	**0.003**	**≪ 0.001**
CC-NS 24 hr	0.135	**0.003**	**≪ 0.001**
NC-NS 24 hr	0.107	**< 0.001**	**≪ 0.001**